

**PHOTOACOUSTIC METHOD FOR NONDESTRUCTIVE  
TESTING OF CERAMIC BALL BEARINGS**

By

**GORDON H. MILLER**

**Bachelor of Arts**

**Maryville College**

**Maryville, Tennessee**

**1979**

**Submitted to the Faculty of the  
Graduate College of the  
Oklahoma State University  
in partial fulfillment of  
the requirements for  
the Degree of  
MASTER OF SCIENCE  
May, 1994**

PHOTOACOUSTIC METHOD FOR NONDESTRUCTIVE  
TESTING OF CERAMIC BALL BEARINGS

By

GORDON H. MILLER

Bachelor of Arts

Maryville College

Maryville, Tennessee

1979

Submitted to the Faculty of the  
Graduate College of the  
Oklahoma State University  
in partial fulfillment of  
the requirements for  
the Degree of  
MASTER OF SCIENCE  
May, 1994

## ACKNOWLEDGMENTS

I wish to express my sincere gratitude toward Dr. Jerzy Krasinski for enriching my abilities in the laboratory and serving as an example of how to successfully approach and resolve a research effort. I thank him for providing an invaluable experience by allowing me a great deal of freedom while remaining aware of my progress and providing guidance when I needed it. I thank Dr. Ray Zaroni for providing me with instruction and guidance. I thank Dr. X. Xie and Dr. Jim Wicksted for serving on my committee. I am particularly thankful toward my wife, Dr. Helen Miller, who provided me with the encouragement, advice, and support I need throughout my graduate studies. I also wish to express my appreciation for my parents' support, encouragement and sacrifice.

This project was funded by DARPA under contract number F33615-92-5933.

## TABLE OF CONTENTS

Chapter	Page
I. INTRODUCTION.....	1
Nondestructive Testing for Ceramics.....	1
Photoacoustic Spectroscopy.....	3
Photoacoustic Microscopy.....	3
Goal of Thesis.....	5
II. PHOTOACOUSTIC MICROSCOPY AS A NONDESTRUCTIVE TEST OF CERAMIC MATERIAL.....	6
Introduction.....	6
Optical Acoustic Imaging.....	8
Thermal Acoustic Imaging.....	9
Ultrasonic Acoustic Imaging.....	9
Summary.....	10
III. EXPERIMENTAL CONSIDERATION IN PERFORMING PHOTOACOUSTIC MICROSCOPY.....	11
Excitation Source.....	11
Detector.....	11
Depth of Observation & Thermal Resolution.....	12
Optical Resolution.....	13
Adhesive.....	13
Resonance.....	15
The Lock-In Amplifier.....	16
Noise.....	17
IV. THE PHOTOACOUSTIC MICROSCOPE SYSTEM.....	19
Excitation Source.....	19
Sample Preparation.....	21
Signal Generation and Data Collection.....	21
Reduction of Noise.....	22
Resonance.....	23
V. OPTIMIZATION OF PHOTOACOUSTIC MICROSCOPE.....	25
Data Collection.....	25
Optical Effects.....	26
Electrical Effects.....	30
Vibrational Isolation of the Detector.....	34
VI. RESULTS.....	42
Noise Levels.....	42
Reproducibility.....	43

Chapter	Page
VII. ALTERNATIVE DETECTION METHODS.....	48
Introduction.....	48
Michelson Interferometer.....	48
Infra-Red Monitor.....	51
VIII.SUMMARY.....	54
BIBLIOGRAPHY.....	55
APPENDIX A.....	57

## LIST OF TABLES

Table	Page
I. Thermodynamic characteristics of $\text{Si}_3\text{N}_4$ .....	13

## LIST OF FIGURES

Figure	Page
1. Variation of thermal diffusion length as modulation frequency changes .....	14
2. Block diagram of experiment used to generate and detect the PA signal.....	20
3. Frequency response of sample/detector element.....	24
4. The noise level as measured by the lock-in amplifier changes as the pause time between the motor stopping until the computer begins sampling the PA signal.....	27
5. An experiment performed on a dark, absorbing grain of the ceramic material.....	28
6. An experiment performed on a light, reflective grain of the ceramic material.....	29
7. A scan was made while the laser warmed up resulting in a ramping of the PA signal as the output of the laser increased from 50 to 65 mW.....	31
8. The first of two scans, this and the next figure shows a decaying background signal indicative of a capacitive piezo discharging. A resistor placed between the electrodes of the sample holder stabilized the baseline.....	32
9. The second of two scans, this and the previous figure shows a decaying background signal indicative of a capacitive piezo discharging.....	33
10. A scan made prior to floating the optical table.....	36
11. An experiment performed after floating the optical table showing a reduction in noise of more than two orders of magnitude.....	37

Figure	Page
12. In this experiment the heat exchanger was turned on midway through but no water flowed through the laser head. The noise is indicated by the dashed lines.....	38
13. In this experiment the heat exchanger was turned off midway through as water flowed through the laser head. Note the increase in noise produced by the water flow as indicated by the dashed lines.....	39
14. The heat exchanger's pump was turned on while the detector was enclosed within a box with no acoustic dampening material present.....	40
15. The heat exchanger's pump was running and was shut off midway through this experiment. The detector was enclosed within a box with acoustic dampening material present.....	41
16. Experiment performed after optimizing isolation of the photoacoustic system.....	44
17. Experiment performed prior to optimizing isolation of the photoacoustic system.....	45
18. Experiment performed to test for addition of noise into photoacoustic system from electrical sources.....	46
19. Three scans over a region of ceramic material to verify reproducibility of photoacoustic scans.....	47
20. Block diagram of Michelson Interferometer used to detect photoacoustic signal.....	52
21. Diagram of fringe intensity as length of interferometer arm changes.....	53



## CHAPTER I

### INTRODUCTION

#### Nondestructive Testing for Ceramics

Often, advancement in engineering takes place due to new materials being developed and utilized in industrial applications. The development of  $\text{Si}_3\text{N}_4$  ceramic ball bearings for high temperature engines is an example of an improved performance by the use of a newly developed material. New materials demand new techniques be developed or old techniques be adapted to test their structural integrity and assist in improving manufacturing. Nondestructive techniques applicable to ceramic materials detect flaws that could lead to failure of the material.

Radiography is a nondestructive test that utilizes gamma-rays or x-rays to cast a shadow image of the sample onto a fine grain film. Image enhancement techniques have improved this procedure's performance. Microfocus x-ray used with thin samples (1 to 2.5 mm) can detect flaws on the order of 50 microns [1]. Radiography's sensitivity toward cracks is poor if the crack is tight or if it is aligned in the direction of propagation of the x-ray beam [2].

Ultrasonic nondestructive evaluation utilizes piezo elements as a single emitter and multiple detectors. The

ultrasonic waves are scattered by flaws and discontinuities, and its resolution is determined by the wavelength of the ultrasonic wave. The resulting secondary waves are detected by receivers positioned for inspection in more than one orientation. Scattering occurs at interfaces and boundaries as well as at voids. The technique works best with flat sided parts since more complex shapes complicate the analyses [3].

Fluorescent dyes are useful for observation of surface cracks and flaws. A sample can be coated with a penetrating fluorescent dye and then, after the dye outside of surface cracks has evaporated, microscopic examination under ultraviolet light to reveals cracks the dye has seeped into [4].

Scanning laser acoustic microscopy (SLAM) has successfully detected surface and subsurface cracks and flaws in  $\text{Si}_3\text{N}_4$ . The technique utilizes a piezoelectric transducer as a source of ultrasonic acoustic waves that impinge on a flat sample at an acute angle. A laser is used to scan the ripples generated in a thin metal film coupled to the sample through water. The ripple pattern is changed by any voids, cracks or other flaws being present and altering the density of the sample. Surface cracks of depths of less than one micron were observed, however analysis is complicated if the samples are not flat, highly polished material [5]. The technique is versatile and can be performed in an interference mode to elucidate further information about the density profile of the material being tested [6].

## Photoacoustic Spectroscopy

When a bright beam of light is amplitude modulated (AM) and focused onto a sample, if the light is absorbed, an acoustic signal is produced at the same frequency as the modulation frequency and the strength of the signal varies directly with the absorption of the light by the material or with the intensity of the incident light. If the intensity is monitored and the resulting acoustic signal is normalized to eliminate the effects of such variation, then the resulting signal depends on the absorption of the light by the sample. An absorption spectrum can be produced by monitoring the strength of the acoustic signal generated as the wavelength of the modulated light beam changes. Photoacoustic (PA) spectroscopy is the generation of absorption spectra based on the PA response of the material being tested. PA spectroscopy has been performed on all three states of matter [7-9] and has demonstrated sensitivity of measuring absorption coefficients down to  $10^{-6} \text{ cm}^{-1}$  [10].

## Photoacoustic Microscopy

Sometimes called thermoacoustic imaging, PA microscopy is based on the PA effect when the light beam has been focused down to a few microns in diameter and scanned across an area of the sample. There are three mechanisms which interact in the formation of a PA signal on a microscopic scale. Typically, one of the three mechanisms dominates depending on the characteristics of the sample and of the experiment being

performed. The three mechanisms are [11]

- absorption of light by the sample,
- generation and propagation of heat waves,
- production and propagation of acoustic waves.

Optical PA microscopy can be performed on optically nonuniform materials that have low absorption coefficient. An increase in the amplitude of the PA signal is caused by the light being absorbed more in some areas, for example by an iron filing inside a quartz crystal.

Thermally inhomogeneous materials possess sites that have thermodynamic variations from the rest of the material. Because the sites react differently to heat than the bulk of the sample, there is a change in the magnitude of the PA signal when the light is focused within one thermal diffusion length of the anomaly. The resolution of this technique is determined by the thermal diffusion length which, in turn, is determined by the thermodynamic characteristic of the sample and the modulation frequency of the light beam. Opaque samples can undergo thermal PA microscopy instead of optical PA microscopy.

Acoustic PA microscopy requires ultrasonic frequencies because the resolution of the technique is determined by the acoustic wavelength. In most solid material the acoustic frequency must be on the order of GHz to achieve a resolution of several microns.

PA microscopy performed at frequencies in the 10 Hz to 10 KHz range is based on thermal effects and possesses the required resolution to detect flaws that endanger the

structural integrity of  $\text{Si}_3\text{N}_4$  ceramics such as ball bearings. These subsurface structures lead to catastrophic failure of the ball bearing. Due to the opaque nature of the ceramic material, optical inspection is inadequate for detecting the voids and cracks that are produced during the manufacturing of the ball bearings. Radiography requires thin samples for micron resolution and is not useful for objects greater than a couple of millimeters in thickness. Curved surfaces such as ball bearings make analysis by ultrasonic techniques difficult [12].

#### Goal of Thesis

The goal of this study is a proof of principle to show the feasibility of using the PA technique operating at the resonance frequency of the detector/sample structure. A review of the current literature on using thermal PA microscopy as a nondestructive testing technique for ceramic material has been made. An experimental apparatus for the study of this effect has been constructed and testing has been done; the results are presented herein.

## CHAPTER II

### PHOTOACOUSTIC MICROSCOPY AS A NONDESTRUCTIVE TEST OF CERAMIC MATERIAL

#### Introduction

Photoacoustic microscopy (PAM) is the use of a well-focused modulated beam of light, typically a laser beam, to generate an acoustic wave in a sample. The PA effect was first reported by A. G. Bell in 1880 [13]. Bell used sunlight since the source of radiation and a carbon microphone as a detector. The resulting signal was very weak and interest in the effect quickly died away. The effect is weak since less than one ppm of the absorbed optical energy is converted to acoustic energy [14]. The recent increase of interest in the PA effect derives from the advent of intense light sources (e.g. lasers and arc lamps), sensitive acoustic detectors (e.g. microphones, hydrophones, and piezo elements), the unique applications (e.g. spectroscopic studies of opaque materials) of PA, and the sensitivity of PA spectroscopy [15].

Absorption of intensity-modulated radiation anywhere on the sample results in a periodic, localized heating of the sample. Two mechanisms transmit this energy to the surrounding media. The first type of energy transfer is the heating of the immediate area by means of heat diffusion and conduction. The rate of heat transfer via this mechanism

depends on the thermal diffusivity,  $\alpha$ , of the material. The thermal diffusivity is described as:

$$\alpha = k / C \rho \quad (1)$$

Where  $k$  is the thermal conductivity,  $\rho$  is the density of the material, and  $C$  is the specific heat. When the heating is periodic at frequency  $\omega$ , then the distance of appreciable heat transfer into the sample media is given by:

$$\mu = (2 \alpha / \omega)^{1/2} \quad (2)$$

Where  $\mu$  is the thermal diffusion length [16]. The thermal diffusion length determines the resolution of PAM for subsurface flaws in opaque samples at modulation less than ultrasonic. Experimental results have indicated resolution for surface flaws to be on the order of the spot size of the focused laser beam [17].

The second type of energy transfer is a coupling of localized heat energy and the vibrational modes of the material itself. This is generally a nondissipative, thermoelastic process. Below ultrasonic frequencies, the distance over which the thermoelastic energy is transferred is limited solely by the dimensions of the sample or by some boundary conditions, and the speed of the transfer is determined by the speed of sound in the material [16]

The effect of sound-wave generation within solids under laser radiation was first observed by White [18] in 1963.

This effect, when coupled with methods to detect the sound wave and produce a well-focused intense beam of light, is utilized to produce PAM. The PAM technique is useful when utilized as a scanning technique. The two methods of generating a scanning PAM device are to move the sample under the laser beam or scan the laser beam over the sample.

The main physical processes responsible for PAM are:

- radiation absorption which produces
- the generation and propagation of heat waves resulting in
- the production and propagation of acoustic waves.

In principle, all three processes provide information about the microstructure of the sample being scanned due to nonuniformities of the materials optical, thermal and acoustic properties. In practice, the interaction between the sample, the light, and the acoustic frequency at which the light is modulated determines which process is dominant [19].

#### Optical Acoustic Imaging

A sample that is thermally and acoustically uniform and has an optical absorption depth sufficiently large so as to allow effective beam penetration of the sample, may possess centers of optical density that differ from the surrounding sample. These centers would produce a change in the absorption of the light and would be detected as a change in the PA signal. The depth of optical penetration is proportional to the optical absorption depth [20].



### Thermal Acoustic Imaging

Thermally inhomogeneous samples can be opaque and the thermal diffusion length determines the resolution of the PAM as well as the sampling depth. The inhomogeneity of the material produce nonuniform heating of the sample within the volume determined by the thermal diffusivity (see equation 1), even though the optical power absorbed remains constant. These variations are transferred to the acoustic waves which are detected by an attached piezo audio pick-up or by a gas coupled microphone. For analysis of condensed media the thermal diffusion length varies from about 1 mm to about 1  $\mu$ m as the modulation frequency varies from 10 Hz to 1 MHz [21].

### Ultrasonic Acoustic Imaging

Ultrasonic waves can be used to detect anomalies within certain materials. Acoustic nonuniformities are spatial variations that alter the formation and/or propagation of sound (e.g. altered heat expansion coefficient, elasticity constants, velocity of sound, etc.). Such anomalies produce nonuniform excitation of acoustic waves in the volume of light/material interaction and alter the amplitude and phase of the acoustic wave once it has formed. When the effect depends on the formation of the acoustic wave, the thermal diffusion length is an important consideration in determination of the resolution. However, propagation of the sound through the sample media is affected by structures larger than the wavelength of the acoustic wave. The

resolution of a 1 MHz acoustic wave is on the order of 3 to 6 mm. The upper limit of the acoustic frequency is on the order of a few GHz and is determined by the attenuation of the wave by the medium. An acoustic wave with a frequency of a few GHz has a resolution of several  $\mu\text{m}$  [22].

#### Summary

For  $\text{Si}_3\text{N}_4$  ceramic material, thermal wave microscopy produces the most informative PA scan. The grain structure of the ceramic attenuates ultrasonic waves of frequencies high enough to detect 10  $\mu\text{m}$  voids. The material is opaque, thus optical penetration is small when compared to the thermal diffusion length. For these reasons the amplitude modulation frequency of the laser beam is on the order of 50 Hz to 1 KHz and the thermal characteristics of the material are utilized in detection of flaws.

## CHAPTER III

### EXPERIMENTAL CONSIDERATIONS IN PERFORMING PHOTOACOUSTIC MICROSCOPY

#### Excitation Source

Consideration of the absorbance characteristics of the material being tested is of importance when selecting a laser source to induce the PA effect. The greater the absorbance of the exciting light by the test material, the greater the strength of the acoustic wave.

The  $\text{Si}_3\text{N}_4$  ceramic is a dark, opaque material that absorbs light of blue as well as red wavelengths. The power that can be introduced to the samples is limited by the Curie point of the piezo detector. If the temperature of the piezo exceeds the Curie point, the microscopic polarized ferroelectric domains in the polycrystalline piezoceramic randomize their polarization, which ruins the detector. The laser is limited to operating at power levels below those that overheat the piezo.

#### Detector

Commonly, the PA signal is detected by either of two methods, the gas-coupled microphone or the piezo element

detector attached directly to a condensed sample [22]. For condensed material such as metals and ceramics, the piezo element offers advantages over gas-coupled microphones [23]. The mismatch in acoustic impedance that results in poor transference of acoustic energy from a solid to a gas then to a microphone is overcome by attaching a piezo element directly to the solid sample. Piezo elements offer superior frequency response over microphones, which is important when utilizing a pulsed excitation of the sample where the pulse widths may be small and result in a high frequency acoustic signal [24].

#### Depth of Observation and Thermal Resolution

The depth of observation and the resolution of the thermal wave imaging is determined by the thermal diffusion length. The thermal diffusion length is set by selection of the AM frequency of the laser beam and is about 100  $\mu\text{m}$  at 100 Hz [25]. The thermal diffusion length is found by equation 2. Table I gives the values of the significant thermodynamic constants and the resulting thermal diffusion length for  $\text{Si}_3\text{N}_4$ . At 325 Hz, the thermal diffusion length is 114  $\mu\text{m}$ . Figure 1 illustrates the change of the thermal diffusion length vs modulation frequency.

detector attached directly to a condensed sample [22]. For condensed material such as metals and ceramics, the piezo element offers advantages over gas-coupled microphones [23]. The mismatch in acoustic impedance that results in poor transference of acoustic energy from a solid to a gas then to a microphone is overcome by attaching a piezo element directly to the solid sample. Piezo elements offer superior frequency response over microphones, which is important when utilizing a pulsed excitation of the sample where the pulse widths may be small and result in a high frequency acoustic signal [24].

#### Depth of Observation and Thermal Resolution

The depth of observation and the resolution of the thermal wave imaging is determined by the thermal diffusion length. The thermal diffusion length is set by selection of the AM frequency of the laser beam and is about 100  $\mu\text{m}$  at 100 Hz [25]. The thermal diffusion length is found by equation 2. Table I gives the values of the significant thermodynamic constants and the resulting thermal diffusion length for  $\text{Si}_3\text{N}_4$ . At 325 Hz, the thermal diffusion length is 114  $\mu\text{m}$ . Figure 1 illustrates the change of the thermal diffusion length vs modulation frequency.

Table I: Thermal characteristics of  $\text{Si}_3\text{N}_4$

Thermal Conductivity (cal/cm-s-°C)	Density (g/cm <sup>3</sup> )	Specific Heat (cal/g-°C)	Thermal Diffusion Length (μm) at 100 Hz
0.072	3.18	0.17	206

### Optical Resolution

To generate a well-focused laser beam of a known diameter, a negative lens used in conjunction with an aperture (to eliminate diffraction rings produced) fills the objective lens of the microscope resulting in a focused spot of the size defined by the equation:

$$ss = 2[1.68 \lambda / \text{NA}] \quad (3)$$

In this approximation, the spot size,  $ss$ , is directly proportional to the wavelength,  $\lambda$ , and indirectly proportional to the numerical aperture of the lens,  $\text{NA}$ .

### Adhesive

Matching the acoustical impedance of the sample and the piezo detector results in maximizing the transfer of the acoustic energy. The interface between these two elements should consist of a hard, brittle epoxy to optimize acoustic transfer. This can be achieved by adding extra resin to the epoxy mix and warming the adhesive as it hardens. Some experimentation is required with a particular epoxy to optimize the desired results.

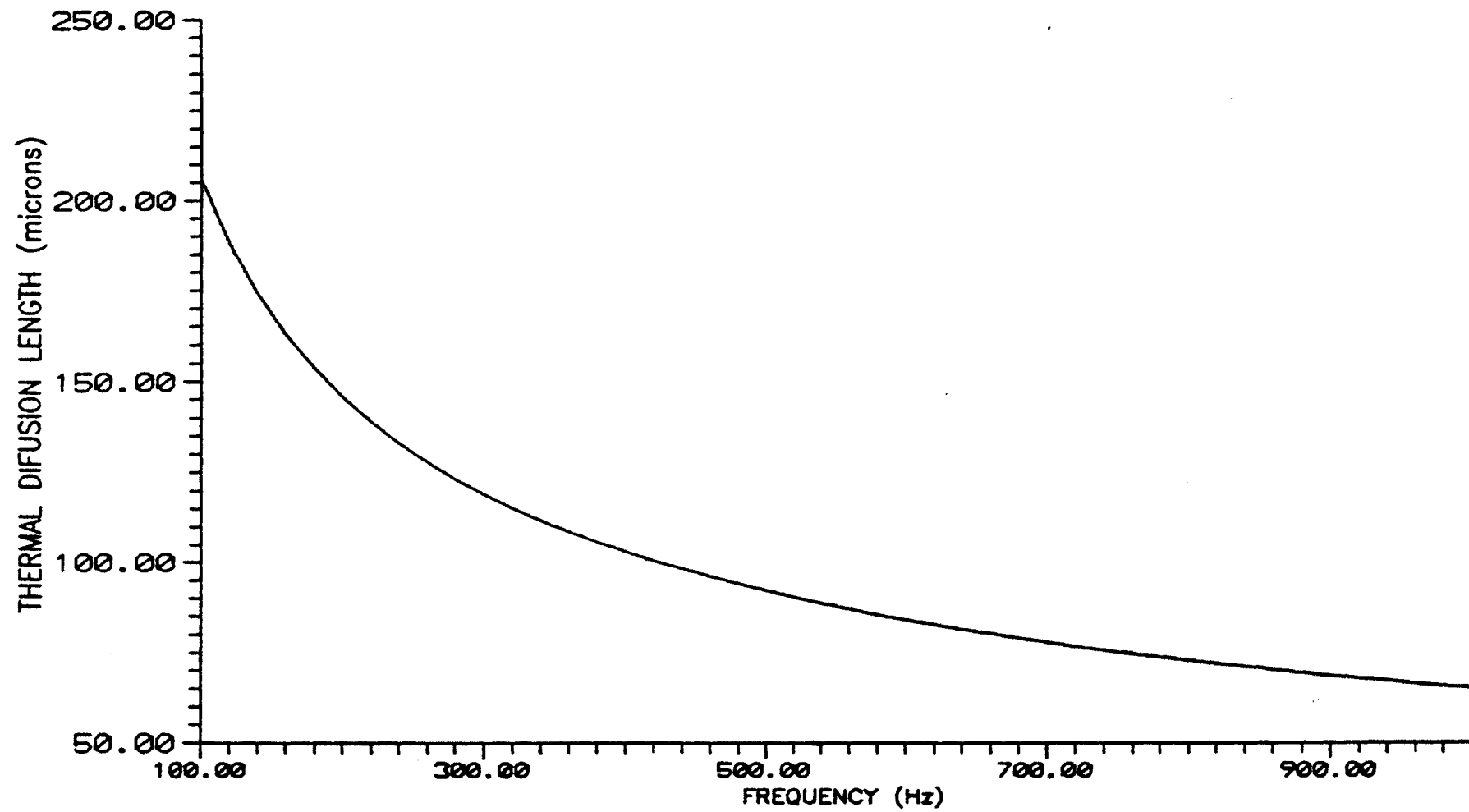


Figure 1. Variation of thermal diffusion length as modulation frequency changes.

## Resonance

Once the sample/detector element is formed, the resonance of the device can be determined. A function generator used with an oscilloscope and a frequency counter provide the means of determining the frequency response of the element. The resonance of the element is useful as a preliminary filter for the PA signal. The detector/sample element can be considered as a damped harmonic oscillator acted on by a harmonic, external driving force. As a damped harmonic oscillator, the element's motion is a result of the interplay of a restoring force and a frictional force. The  $Q$  of the system is a measure of the degree of dampening in the system. A high  $Q$  system is slightly damped and the friction force is much smaller than the restoring force.  $Q$  is defined as:

$$Q = \frac{(m\omega_o)}{f} = \frac{\sqrt{m\cdot k}}{f} \quad (4)$$

where  $m$  is the mass of the oscillator,  $\omega_o$  the natural frequency of the oscillator,  $k$  the force constant of the restoring force and  $f$  the friction factor for the retarding force. The amplitude of the steady state motion of the oscillator acted upon by a harmonic external force is given by:

$$B = \frac{F}{if\omega [1 + iQ(\frac{\omega}{\omega_o} - \frac{\omega_o}{\omega})]} \quad (5)$$



Under conditions where the external force's frequency  $\omega \ll \omega_0$ , then B is approximately:

$$B = \frac{F}{k} \quad (6)$$

At the other extreme where  $\omega \gg \omega_0$ , B is approximated by:

$$B = \frac{F}{m\omega^2} = \frac{F}{k} \quad (7)$$

At the natural or resonance frequency, the steady state amplitude of the displacement of the oscillator is described by:

$$B = \frac{QF}{k} \quad (8)$$

At resonance, the signal generated by the piezo, directly proportional to its displacement, is larger by a factor of Q. The noise in the system is approximated by a white noise model and has the same magnitude at resonance as at other frequencies. For this reason the signal to noise ratio increases at  $\omega_0$  by the factor Q and the resonance of the system acts as a bandpass filter centered on  $\omega_0$ .

#### The Lock-In Amplifier

The PA signal is a small voltage compared to the noise produced in a photoacoustic microscope system. One technique to extract the signal from the noise is to produce and measure

the signal at a selected frequency. The lock-in amplifier performs this task and is capable of measuring nanovolt signals. The amplifier has differential input for the signal source and a reference input to synchronize with the modulator of the excitation source. The reference frequency, supplied by the modulator, determines the frequency for which the amplifier filters. To optimize the filtration, the lock-in has a mixer that shifts the input signal to 0 Hz (DC). This allows for minimizing the width of the bandpass of the filter and optimizing the signal to noise ratio.

All physical processes require time to take place. The amplifier is equipped with electronics that allow phase shifting of the signal. This feature compensates for time differences produced by a delay time between the stimulus arriving to the sample and the arrival of the signal to the lock-in amplifier.

### Noise

It is of importance to eliminate the noise in the PA system. The main sources of noise are electrical and vibrational. The electrical noise can be minimized by using short, double shielded BNC cables between the sample and the amplifier as well as by filtering the power cords of the computer and the amplifier. In some situations, the experimenter may be required to place not only the detector, but also the amplifier and the computer into Faraday cages to block RF-induced electrical noise.

Vibrational noise couples into the detector via two

## CHAPTER IV

### THE PHOTOACOUSTIC MICROSCOPE SYSTEM

#### Excitation Source

Figure 2 illustrates the experimental setup used to detect the PA signal. The Ar-ion laser was a Spectra Physics 171 operating in multiline mode (457.9 - 514.5 nm). Typically, the laser was operated at an output power level of 100 mW, in continuous current mode. Operating at this power level assures not overheating the piezo detector. Diffraction rings were eliminated from the laser beam by using an appropriate negative lens and an aperture. The microscope's focusing objective diameter was measured and the aperture allowed the laser beam to just fill the lens. The 50x lens (NA of 0.75) focused the laser beam to about a 2  $\mu\text{m}$  spot size.

The chopper (Standford Research System, Model SR540) was adjusted to maximize the output of the resonance peak, between 320 to 380 Hz. Phase was then checked and selected for maximum output and then the chopper was reset until frequency and phase were determined to where output was maximized at the resonance peak. The chopper was acoustically isolated from the table by placing it on a brick resting on bubble wrap packaging material. The resulting vibrational mismatch

## Experimental Apparatus

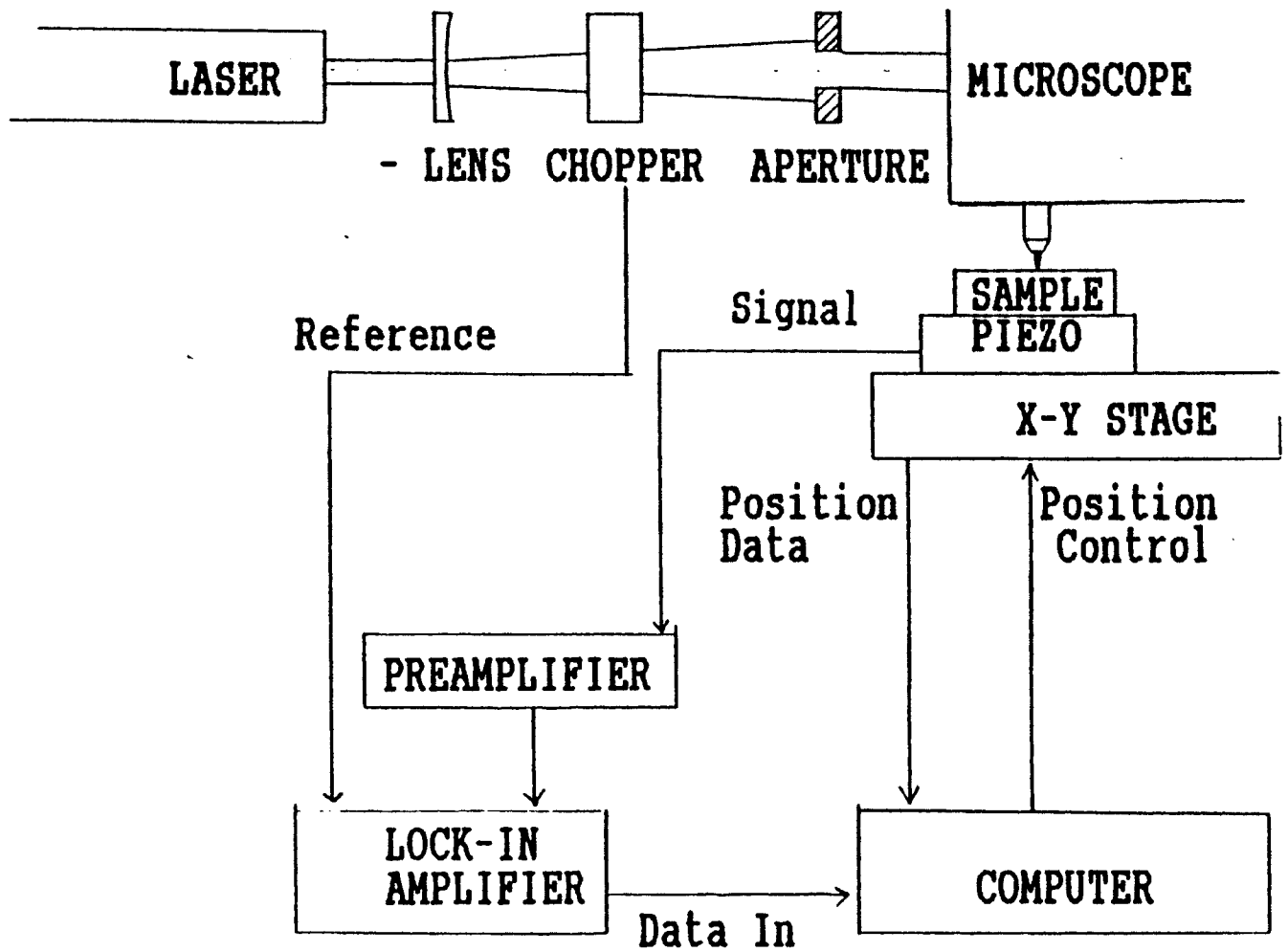


Figure 2. Block diagram of Photoacoustic Microscope

between the materials effectively isolated the chopper.

### Sample Preparation

A diamond saw was used to slice off a section of the  $\text{Si}_3\text{N}_4$  ball bearing. Epoxy was used to attach the section to a piezo ceramic transducer (Piezo Systems, Inc. G-1195 ceramic material). The epoxy was mixed with more resin than the manufacturer had specified and the adhesive was heated to  $80^\circ\text{C}$  for 15 to 20 minutes as it hardened. The resulting bond was rigid and brittle with good acoustical matching with the ceramic detector and sample. The piezo transducer measured 0.75" x 1.5" x 0.020" and was poled for series motor operation. The piezo ceramic material has a density of  $7.5 \text{ g/cm}^3$  and sound velocity of  $0.325 \text{ cm}/\mu\text{s}$  which produces an acoustic impedance of  $2.438 \times 10^6 \text{ g/cm}^2 \text{ s}$ . The  $\text{Si}_3\text{N}_4$  material has a density of  $3.3 \text{ g/cm}^3$  and a sound velocity of  $1.18 \text{ cm}/\mu\text{s}$  [24, 25] which gives an acoustic impedance of  $3.894 \times 10^6 \text{ g/cm}^2 \text{ s}$ .

### Signal Generation and Data Collection

The voltage generated by the detector/sample element was picked up by two electrodes between which the detector was clamped. The lock-in amplifier (Stanford Research Systems, Model SR510) detected the preamplified (Stanford Research Systems, Model SR550) signal at the frequency set by the chopper and delivered an output to the computer (Everex 486-33) proportional to the voltage generated by the detector.

The computer controlled the X-Y stage (Physik

Instrumente, Model M-016.00) and received position data from the DC-Mike drives (Physik Instrumente, Model M-224.00). The computer program used to gather the data sampled the analog/digital (A/D) converter once every 100 ms so the time constant on the lock-in amplifier was set to 100 ms. The control board for the DC motor mikes also contained the A/D converter which simplified data collection. The data file generated contained X-position, Y-position, and the PA signal from the lock-amplifier.

#### Reduction of Noise

The detector/sample element must be acoustically isolated to reduce the noise to an acceptable level. The vibrational noise present coupled into the detector by two routes: direct coupling and air coupling.

Air-coupled noise resulted from sound occurring at the same frequency as the chopping frequency. The detector showed sensitivity to sound such as closing doors, clapping hands, and a variety of others. Although the acoustic impedance mismatch between air and the piezo was high, there was enough energy transferred into the piezo to warrant a sound dampening enclosure to be built about the detector/sample element.

When the sample was firmly fixed to the optical table in order to maximize optical alignment, vibrations were picked up by the table and coupled directly into the detector. The optical table was floated on air-filled pistons that isolated the table from vibrations in the floor, but the table was not anchored in any manner that dampened vibrations present in the

air and so acted as a vibrational antenna, channeling vibrations into the detector. Floating the table reduced the noise level by more than two orders of magnitude, but the detector needed to be acoustically isolated, using a sound barrier composite sheet between the table and the microscope on which the detector was mounted to reduce the noise to an acceptable level.

### Resonance

Sensitivity of the detector was enhanced by operating at the resonance frequency of the sample/detector element. To determine where the resonance frequency occurred, a function generator (Hewlett Packard, Model 3311A1) was attached to the element through a 430 pF capacitor. The frequency was measured by a Tektronix 2236 100-MHz oscilloscope operating as a frequency counter. The voltage generated by the piezo was measured by the oscilloscope referenced to the function generator. Figure 3 shows a typical frequency response curve generated using this method.

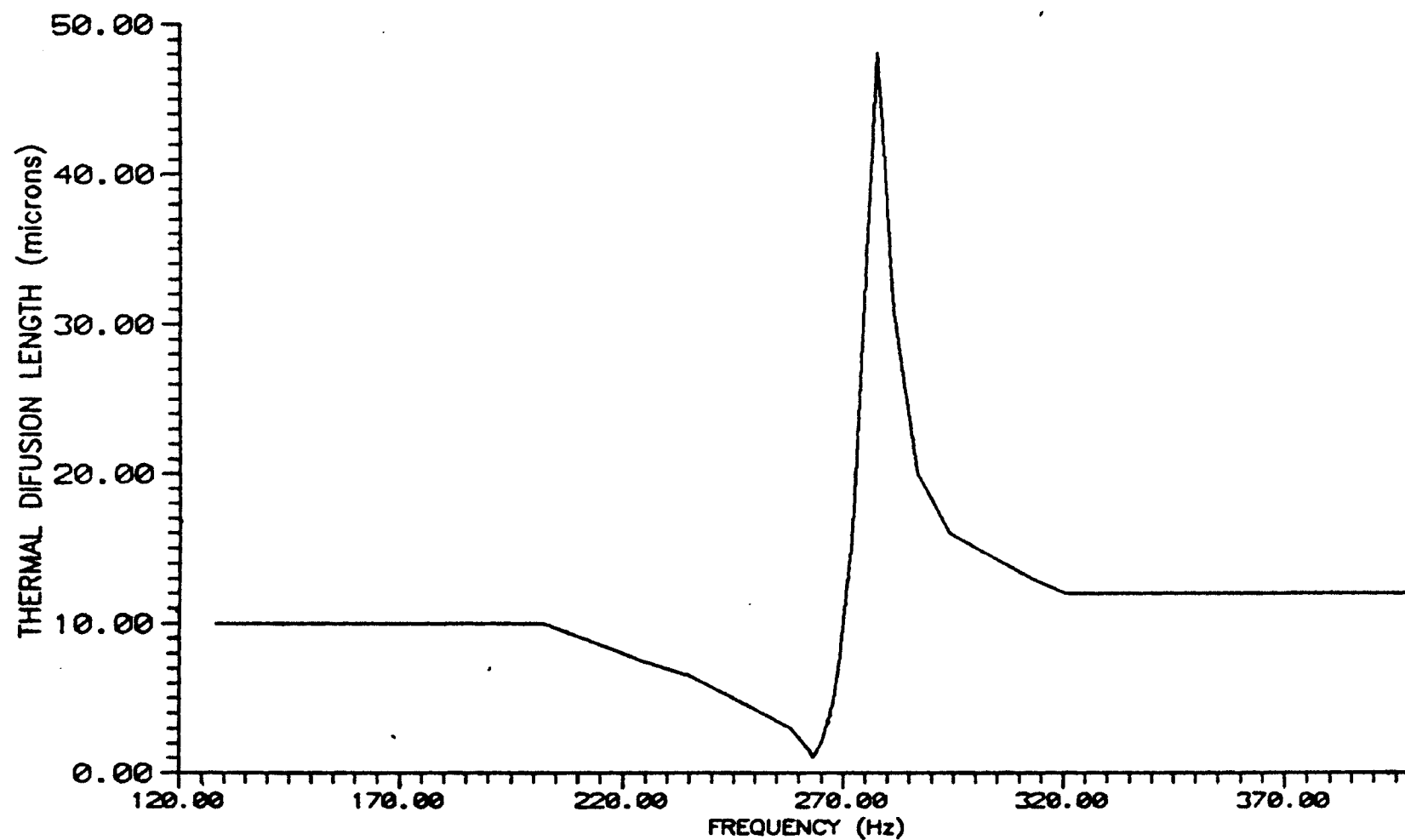


Figure 3. Frequency response of Photoacoustic signal showing parallel and series resonance. FWHM = 7.2 Hz with peak at 276.4 Hz resulting in a  $Q = 38.4$ .



## CHAPTER V

### OPTIMIZATION OF PHOTOACOUSTIC MICROSCOPE

#### Data Collection

The optimization of detection of the PA signal required testing the experimental system under various conditions. The noise was determined by observing fluctuations of the signal at one location on the sample. The laser beam was blocked to generate a zero and then was allowed to stimulate the sample to generate a signal when testing for noise contribution from some variable. The sample was not scanned so that the signal would be free of additional vibrations and so that there would be a constant absorption of the laser beam by remaining on one particular grain of the material. Each data point in any given experiment represents the average of 50 - 10,000 individual samples and there are forty data points. The number of individual samples varies from experiment to experiment but is constant for a given experiment. By increasing the number of samples taken by a factor of ten the noise improved by the square root of ten.

The lock-in is equipped with three electronic filters which, when tested, showed that a reduction in noise occurred when all three were engaged. The dynamic resolution was found

to have very small effects on the noise generated in the PA signal, but the best results were obtained when the dynamic resolution was set to low.

Another technique for reducing the noise in data collection was altering the time between the motor coming to a stop and the start of sampling the PA signal. A comparison of the scans recorded with a 10 s pause and a 15 s pause between a motor halting and the computer beginning sampling the signal showed a large drop in noise level with the longer pause of 15 s. The lock-in was equipped with an option that allowed the noise to be monitored. This option was used to measure the noise as the pause time was varied from 5 - 120 s. The results of this experiment are graphed in Figure 4 and show that the noise decays to a constant value after about a 45 s pause time.

#### Optical Effects

Optical absorption of the laser beam determines the intensity of the resulting PA signal. The surface of the  $\text{Si}_3\text{N}_4$  material has dark areas on a light background when observed under a reflective microscope. The laser beam was focused onto a dark grain and the resulting signal is illustrated in Figure 5. Figure 6 illustrates the result of a measurement made under identical conditions as those shown in Figure 5 except the laser beam is focused onto the reflective background material of the  $\text{Si}_3\text{N}_4$ . Comparison of Figures 5 and 6 show the intensity of the acoustic signal is 10 to 15% stronger for the darker, more absorptive grain. Figure 7

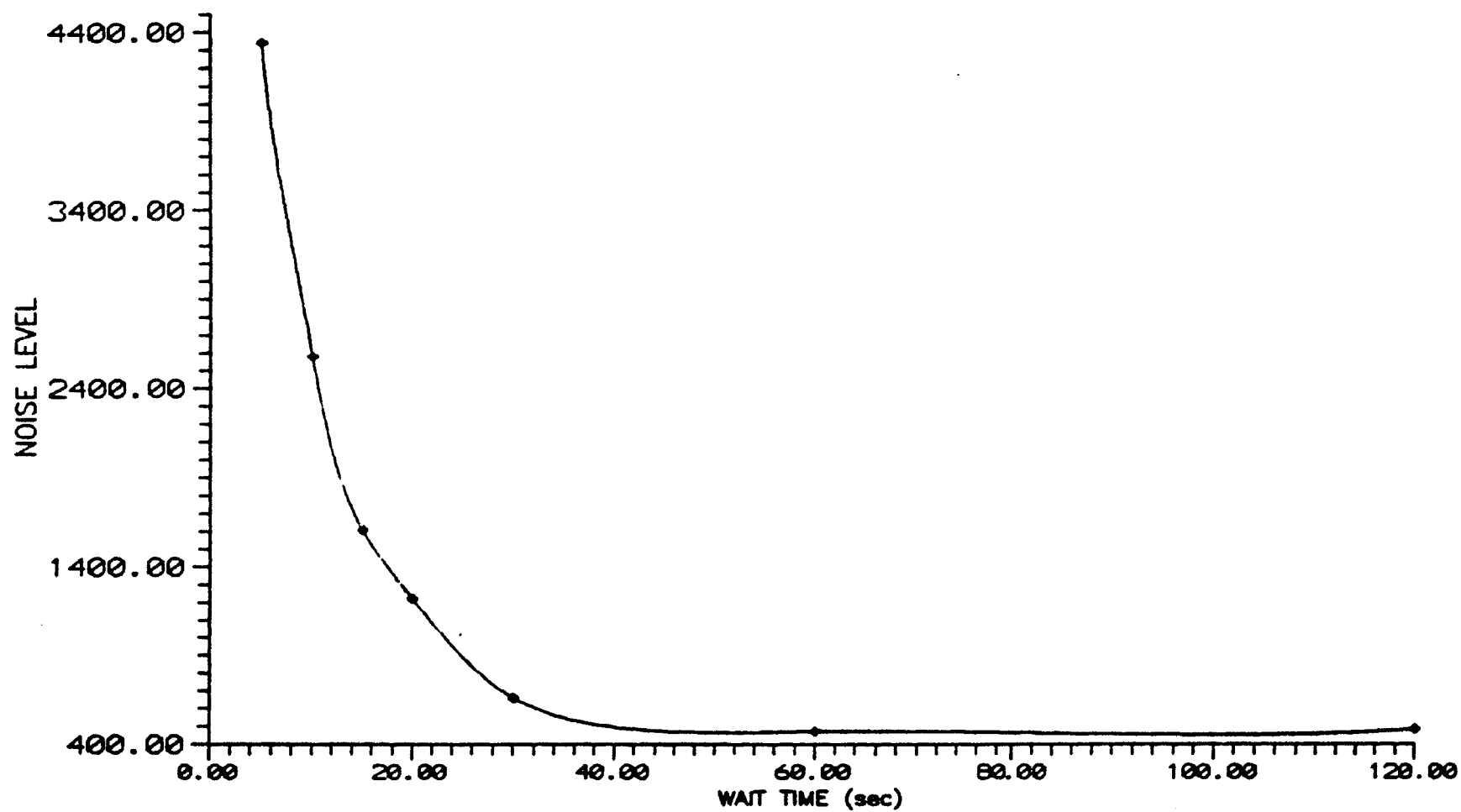


Figure 4. The noise level as measured by the lock-in amplifier changes as the pause time between the motor stopping until the computer begins sampling the PA signal

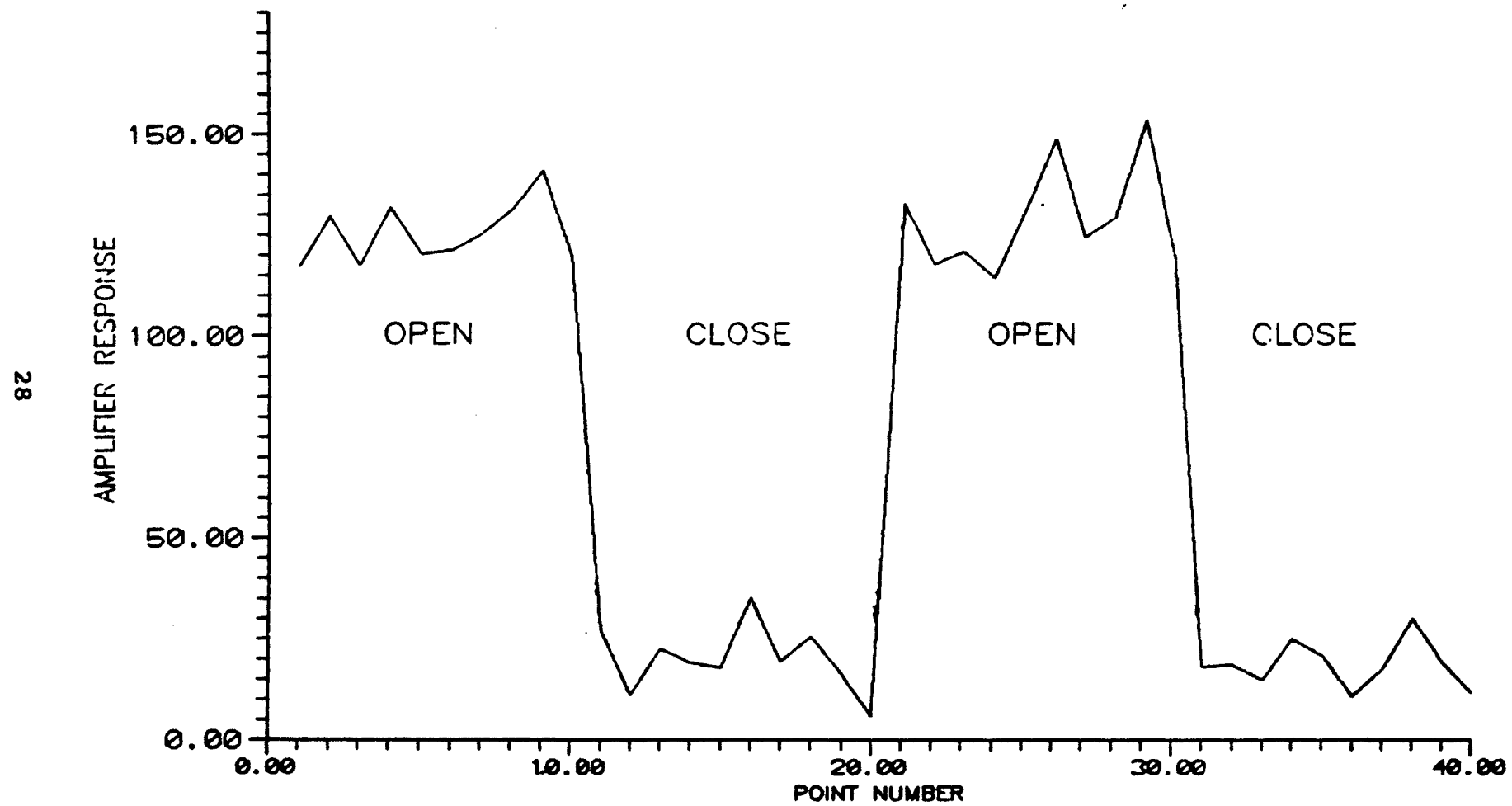


Figure 5. An experiment performed on the dark, absorbing grain of the ceramic material.

illustrates the effect a change in the intensity of the laser has on the PA signal. The measurement was performed during the 15 min warm up period after first activating the laser. The output intensity of the beam ramped from 50 mW up to 65 mW during the time of measurement. The variations in output of the laser is of concern and can be monitored resulting in normalization of the data to compensate for the fluctuations.

The experimenter must be aware of nonuniform optical absorption in the sample when searching for flaws. Optical inspection of the sample surface where a suspected flaw has been located will readily reveal if the effect being measured is due to thermal inhomogeneity, and therefore a flaw, or if there is an optical inhomogeneity influencing the PA signal.

#### Electrical Effects

A significant stabilization of the PA signal was realized when a 330 K $\Omega$  resistor was placed across the electrodes picking up the voltage generated by the piezo element. This resistor allows for the dissipation of the charge collected on the capacitive piezo element. The alternating charging and discharging of the piezo resulted in a drifting baseline as illustrated in Figures 8 and 9. The data collected of the detector/sample element's voltage reveals a decaying baseline. To test for signal distortion the 330 K $\Omega$  resistor was attached in parallel with a piezo element identical to the detector. This structure was attached to a square wave generator and the resulting wave form was observed using an oscilloscope. There was little distortion in the wave form, even with a 200 K $\Omega$

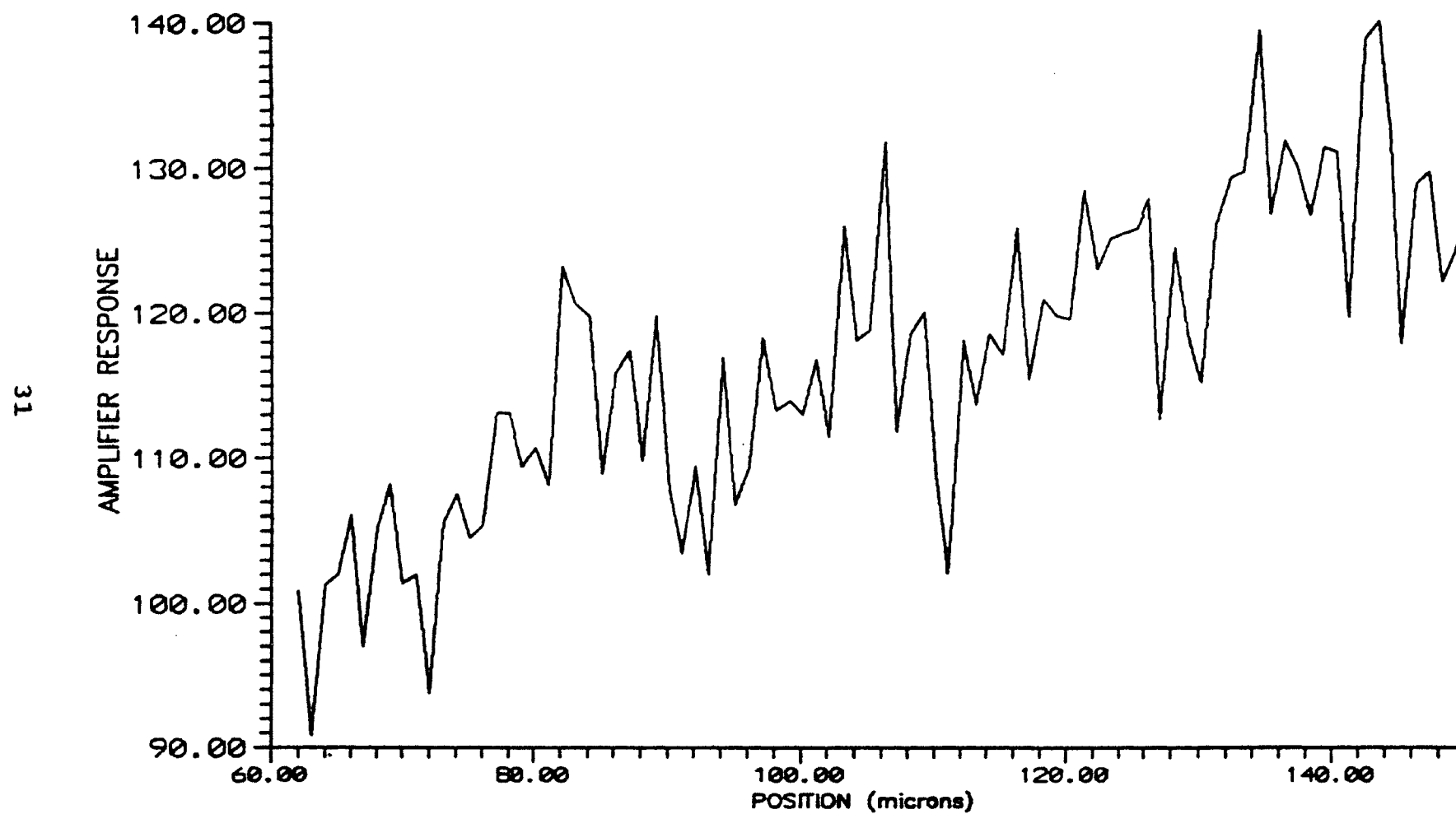


Figure 7. A scan was made while the laser warmed up resulting in a ramping of the photoacoustic signal as the output of the laser increased from 50 mW to 65 mW.

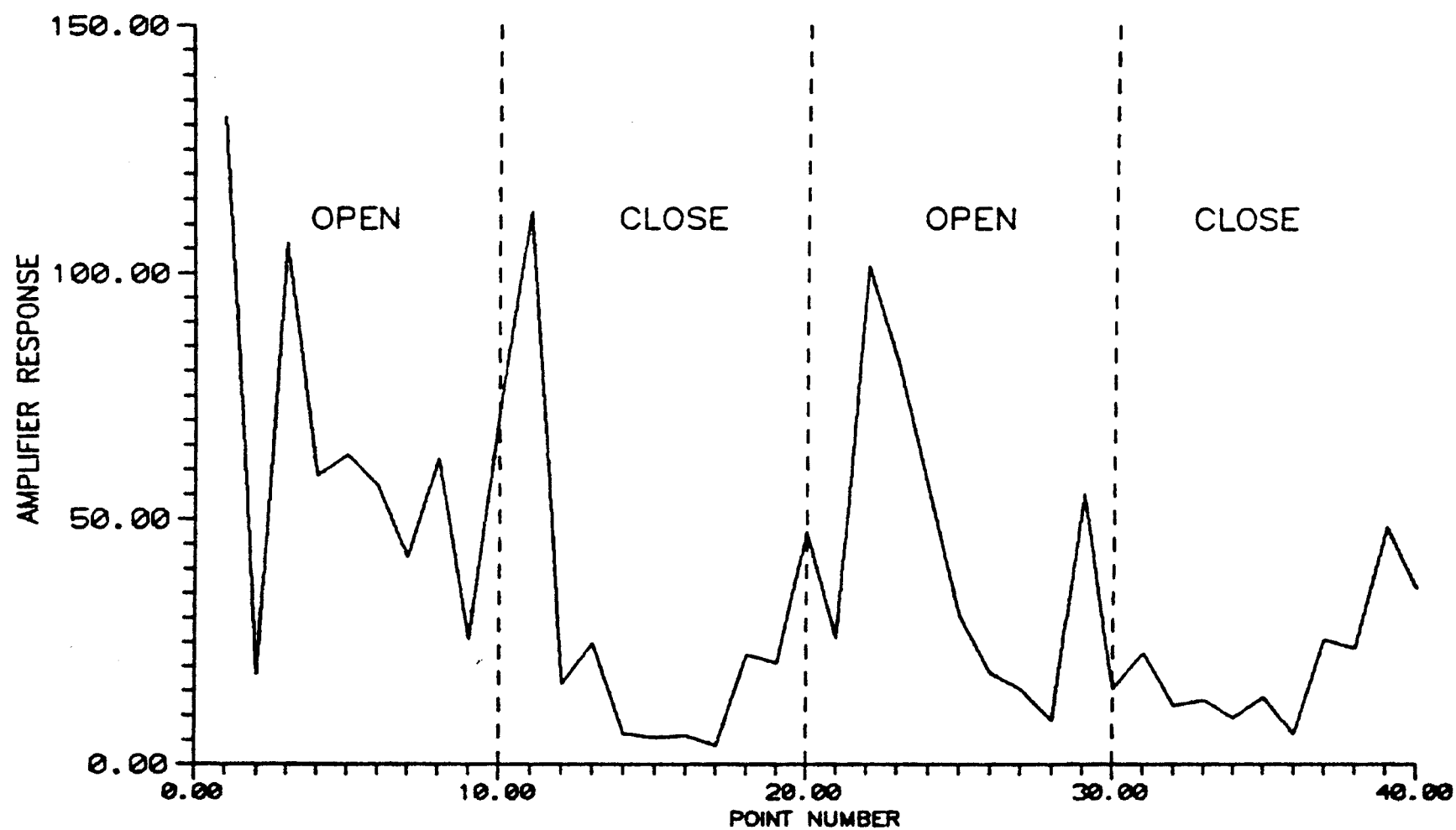


Figure 8. This and the next figure shows a decaying background signal indicative of a capacitive piezo discharging. A resistor placed between the electrodes stabilized the baseline.

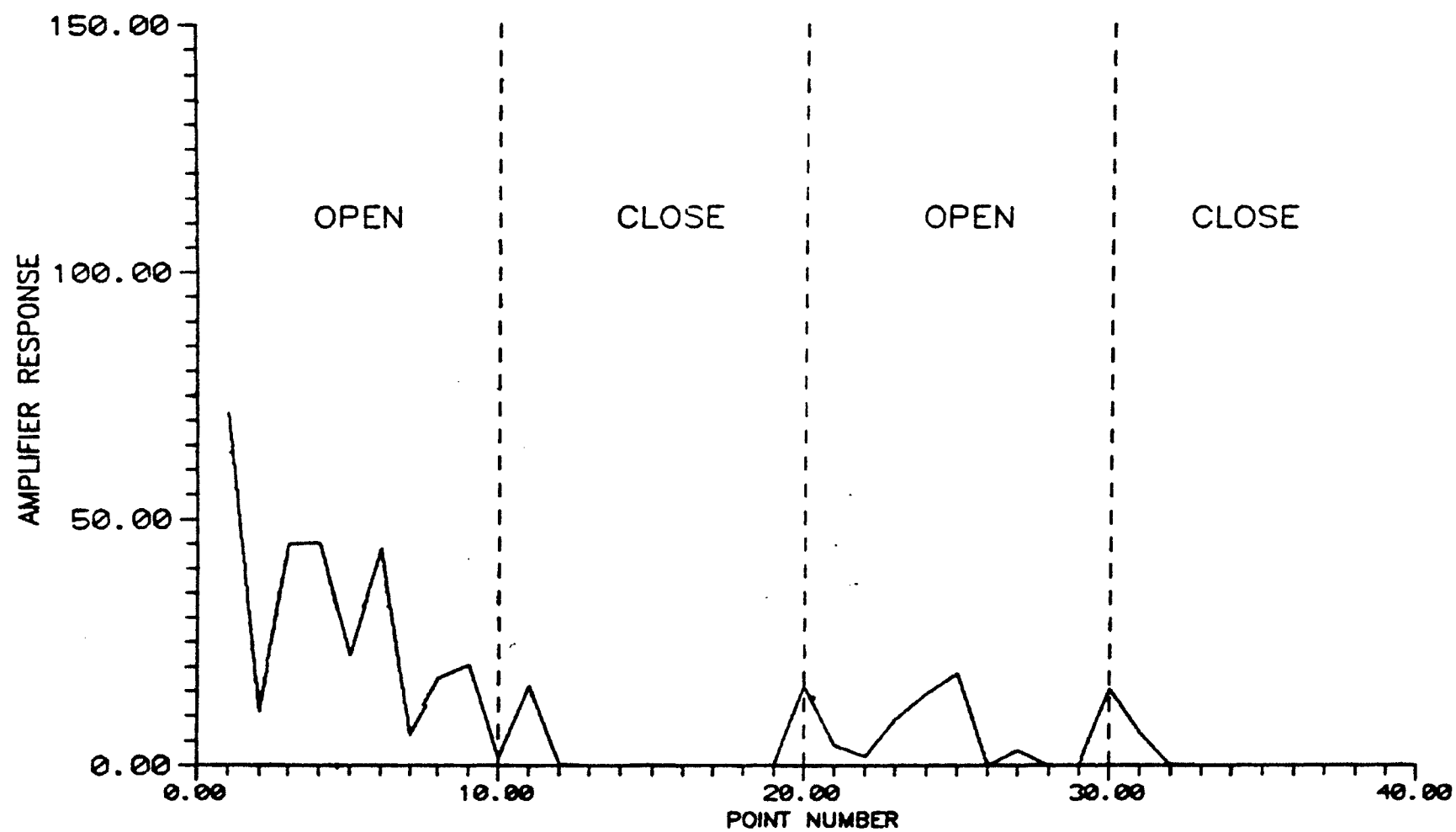


Figure 9. The second of two scans, this and the previous figure shows a decaying background signal indicative of a capacitive piezo discharging.



resistor. The stability of the PA signal was greatly improved with the addition of the resistor.

Various cables were tested by placing them between the detector/sample element and the preamplifier. The double shielded cable transferred the signal with the least noise and was used throughout from detector to lock-in amplifier. Although most of the cables produced little noise, the double shielded cable showed a less erratic behavior over several test scans than the other cables.

A reduction in the electrical noise occurred when line filters were placed on the power cords of the computer and the lock-in amplifier. By using the noise level output of the lock-in, sources of noise could be traced. It was found that prior to placing the line filter on the computer the noise measured by the lock-in increased from 25  $\mu\text{V}$  to 52  $\mu\text{V}$  upon activating the computer. After several improvements were made, including attaching the line filter to the computer (the lock-in amplifier already had one installed), the noise would change from 2.6  $\mu\text{V}$  to 2.8  $\mu\text{V}$  by turning on the computer.

#### Vibrational Isolation of the Detector

The noise introduced into the system by vibrational sources has been detrimental to the observation of small changes in the PA signal. It was found that isolation of the chopper from the table resulted in a reduction of noise in the system. The data illustrated in Figure 10 was collected at a sensitivity setting of 10  $\mu\text{V}$  on the lock-in. Figure 11 shows data collected, at a sensitivity of 100 nV, after the table

was floated on air cushioned pistons. Comparing Figure 10 and 11 illustrates the improvement of the noise level by more than two orders of magnitude.

Floating the table to isolate the experimental system from vibrations in the floor was essential in achieving an acceptable noise level. However, the table and the detector were affected by sound transmitted through the air; the system reacted to closing doors, sounds from adjoining rooms, and music played over the radio. Any vibrations, however generated, showed up in the scan. Figure 12 illustrates the effect starting the recirculating pump of a heat exchanger had on the detector. Note that the water was not flowing into the laser head, which was mounted onto the table. Figure 13 shows further increase in noise when the water was allowed to flow through the laser head. The additional vibrations generated by the water flow coupled into the detector via the optical table.

The coupling of sound into the detector via the air in the room is illustrated in Figures 14 and 15. Figure 14 shows the results of switching on the pump of the heat exchanger without any water flow. The detector was enclosed in a box that had no sound dampening material within it. When the data illustrated in Figure 15 was generated, the box enclosing the detector had been filled with sound dampening material resulted in a decrease in noise coupled into the detector. Sound barrier material was used to line an enclosing plywood box surrounding the detector.

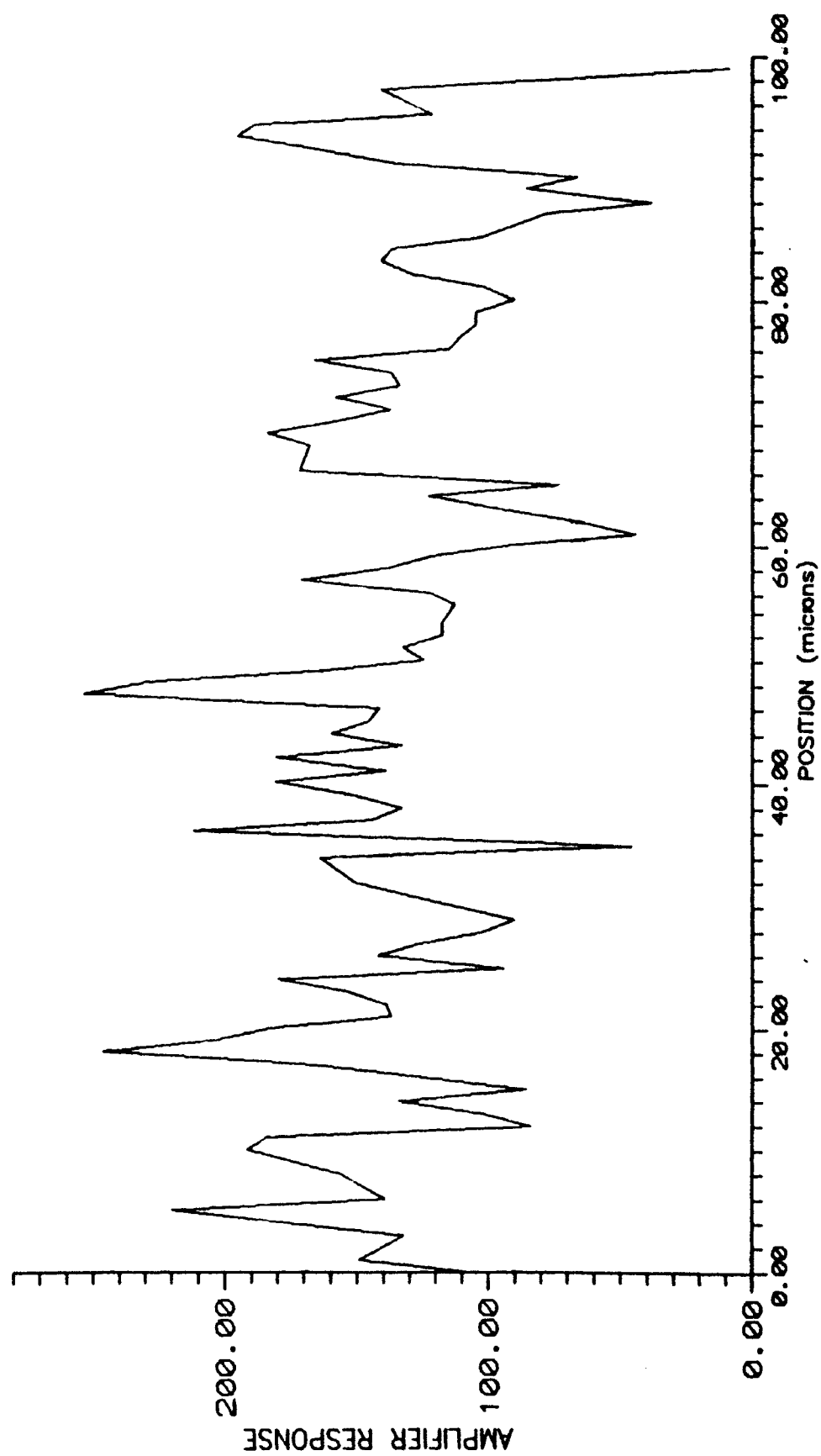


Figure 10. A scan made prior to floating the optical table  
 SENS = 10  $\mu$ V, Jan. 6, 1994.

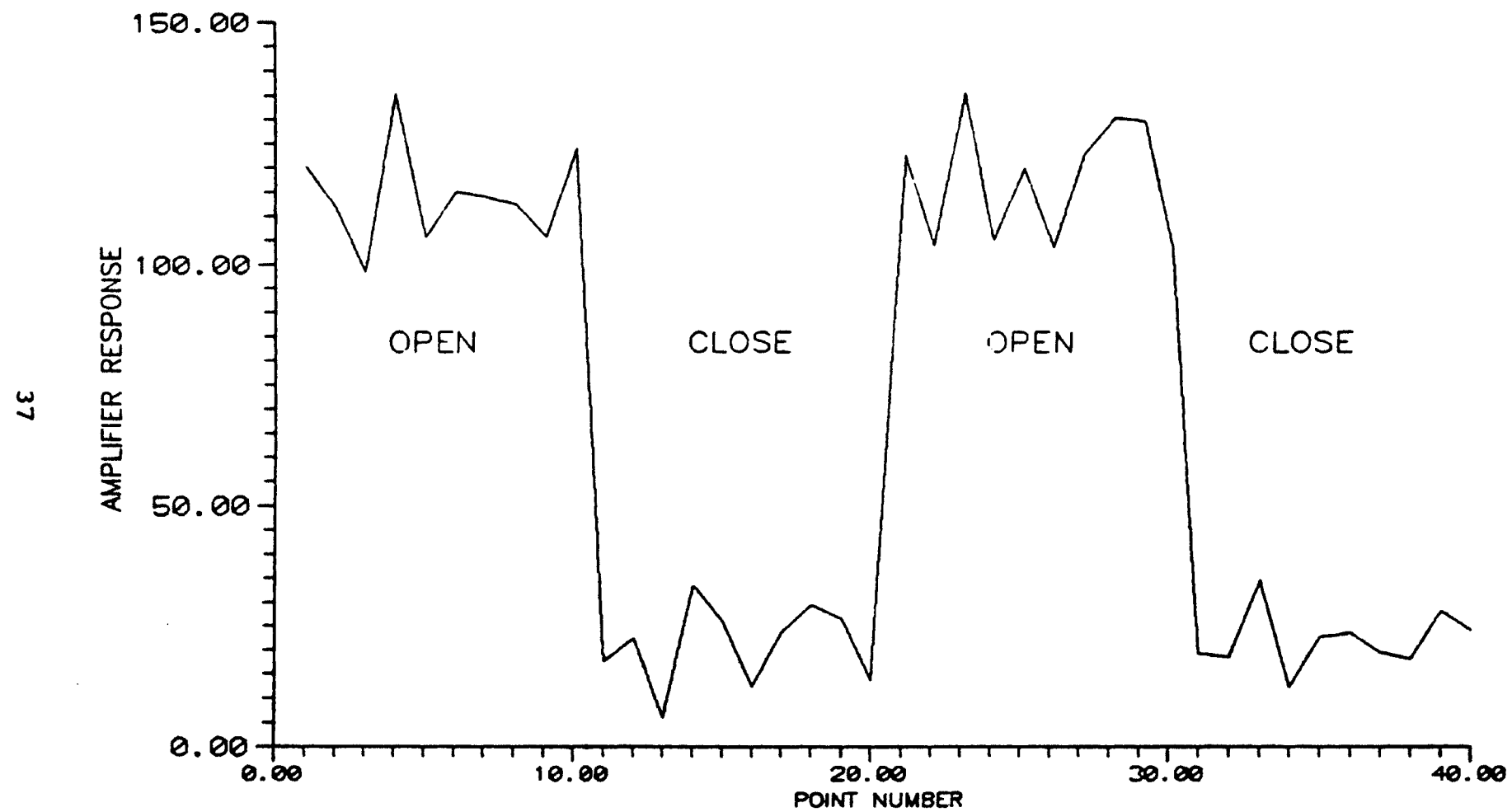


Figure 11. An experiment performed after floating the optical table showing a reduction in noise of more than two orders of magnitude, SENS = 100 nV.

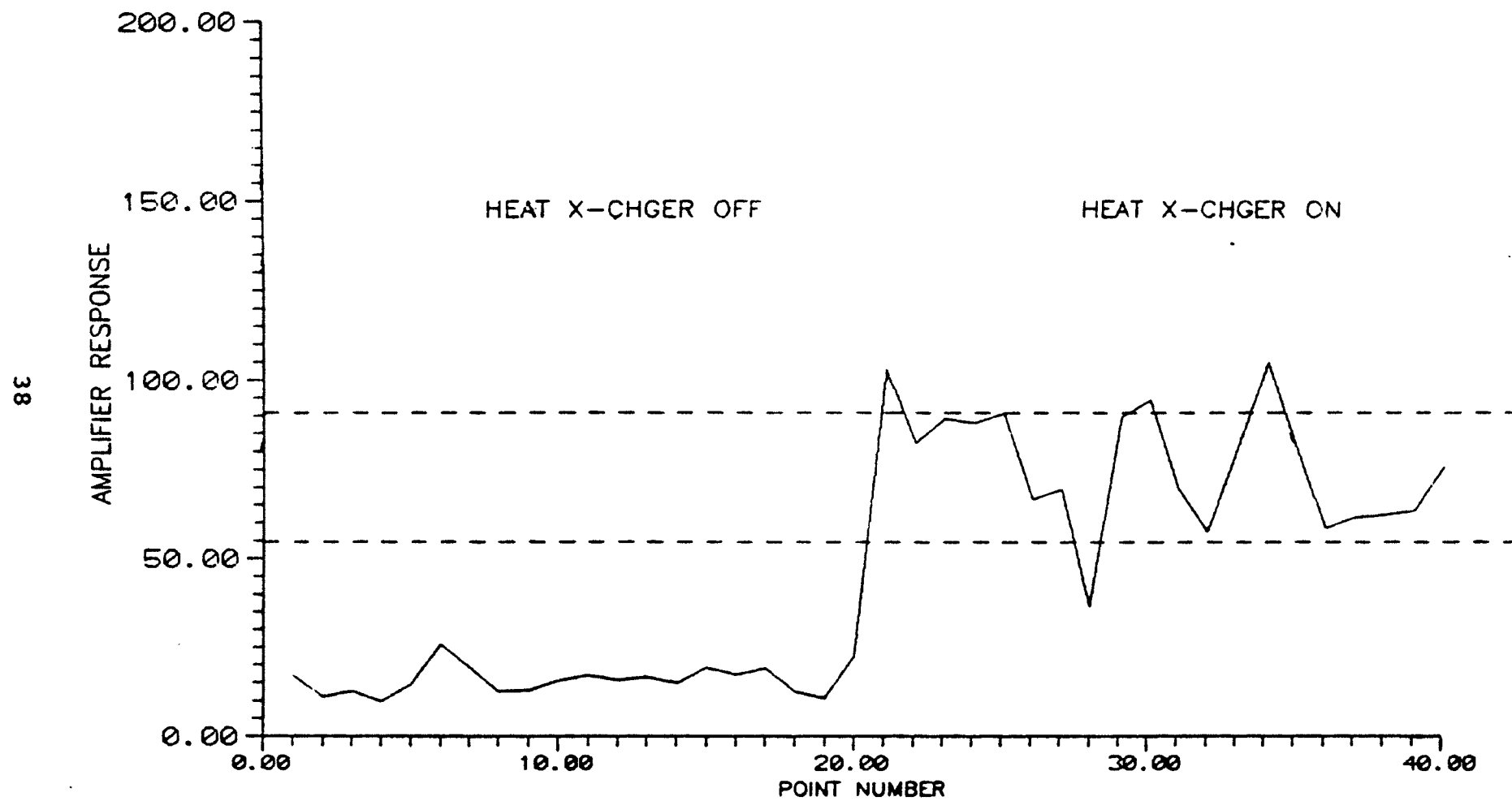


Figure 12. Heat exchanger was turned on midway through but no water flowed through the laser head. The noise is indicated by the dashed lines.

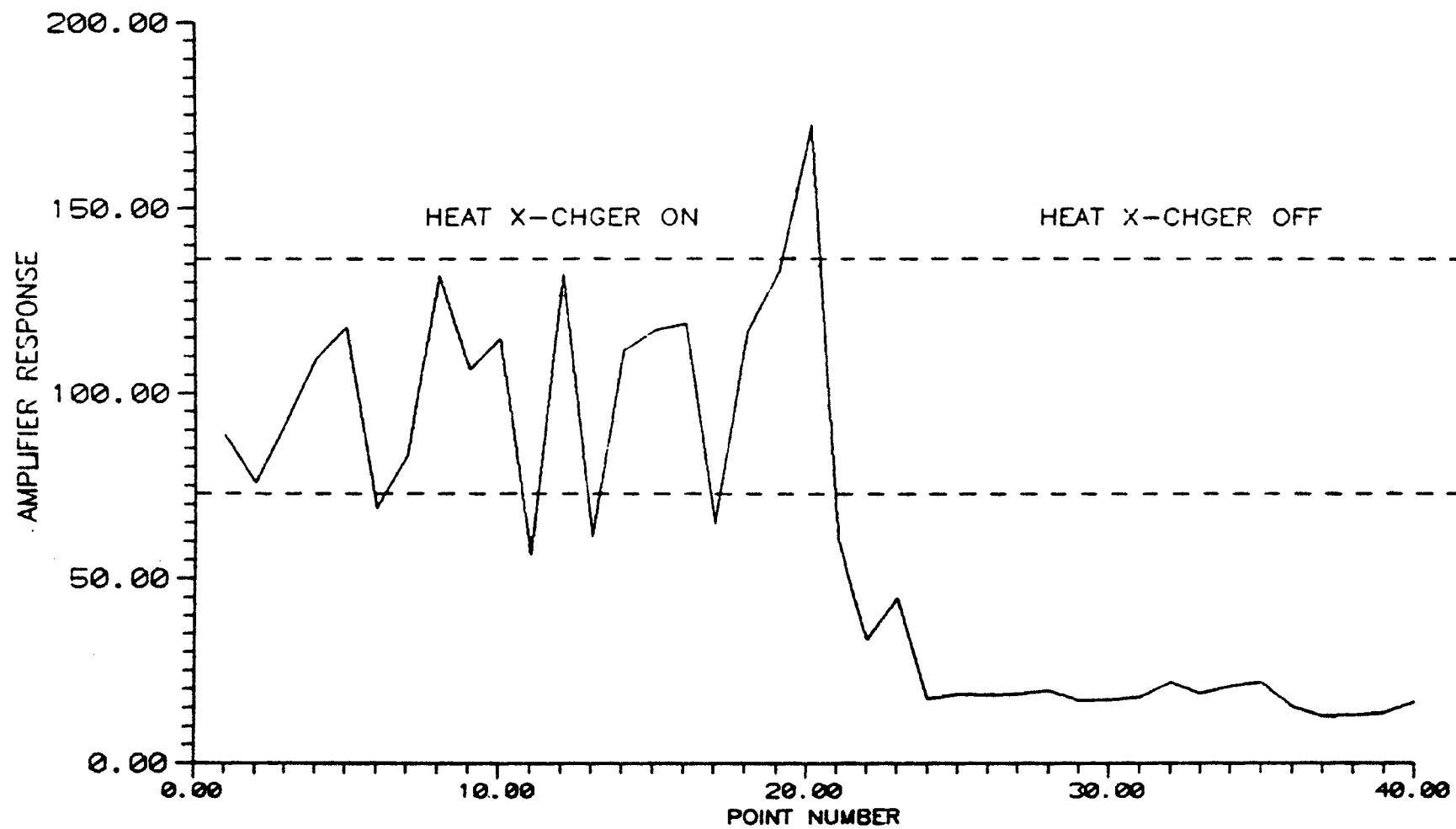


Figure 13. Heat exchanger was turned off midway through as water flowed through the laser head. The noise is indicated by the dashed lines.

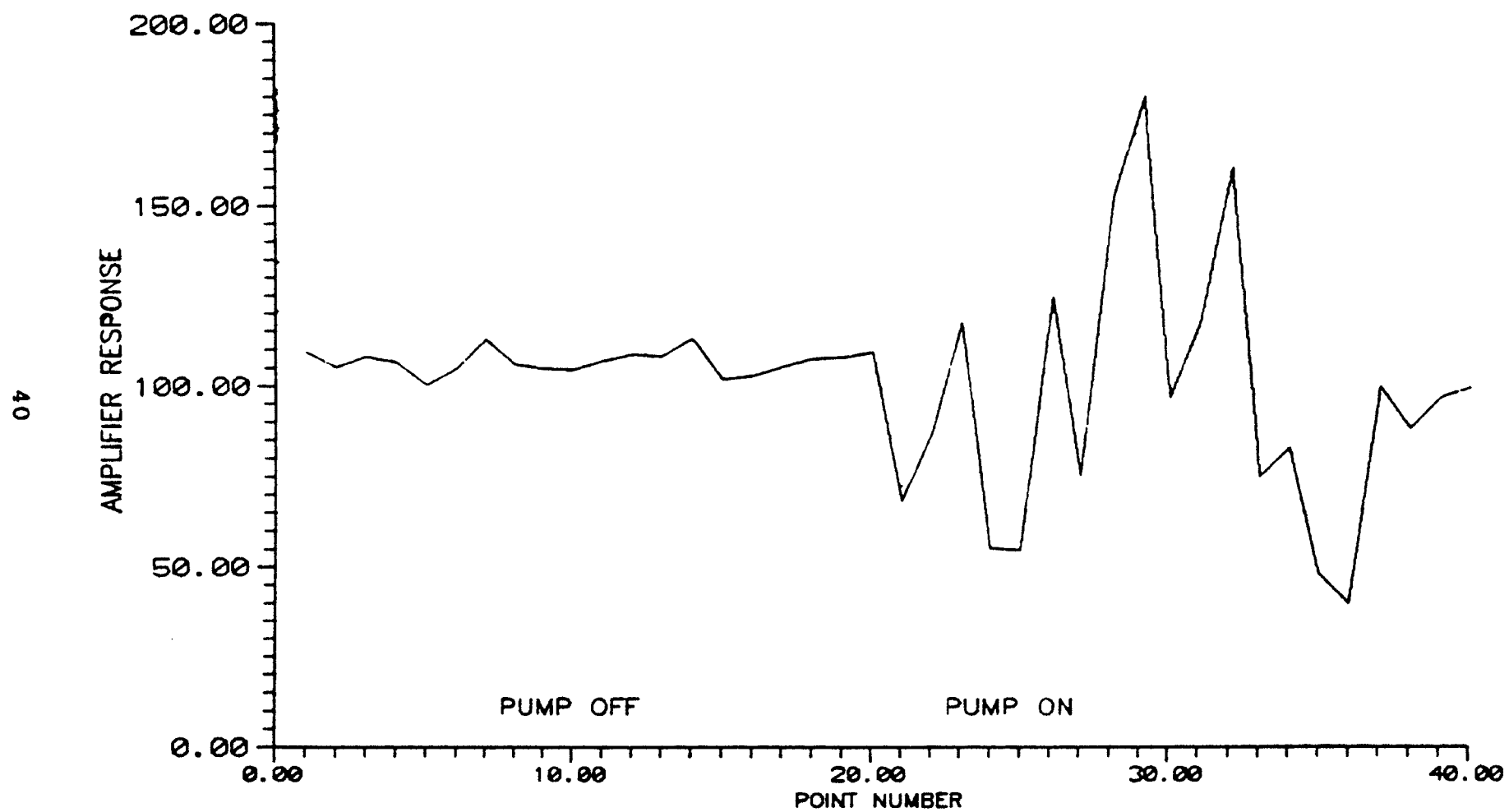


Figure 14. Heat exchanger was turned on while the detector was enclosed within a box with no acoustic dampening material.

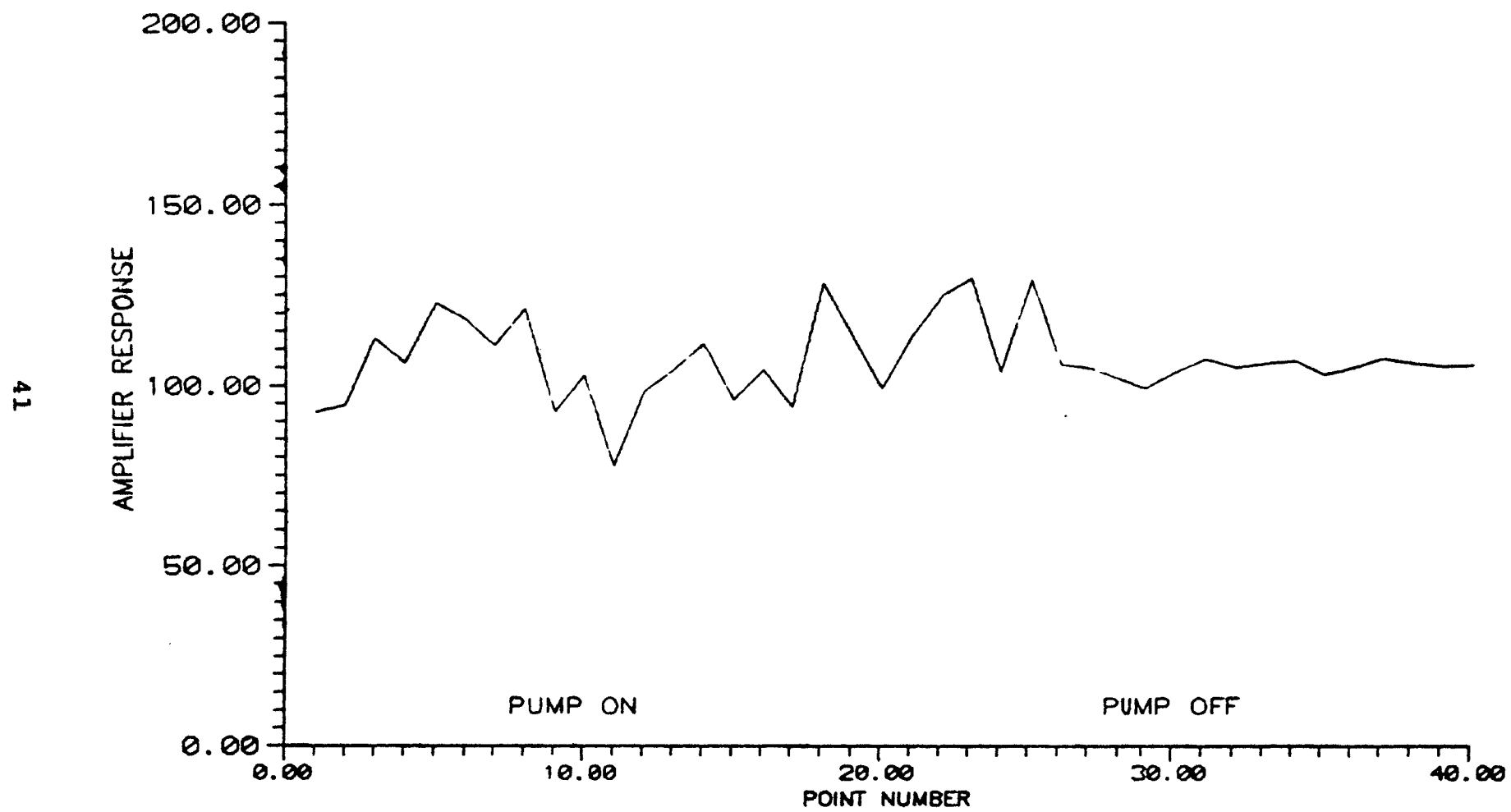


Figure 15. Heat exchanger was turned off while the detector was enclosed within a box with acoustic dampening material.



## CHAPTER VI

### RESULTS

#### Noise Levels

Once the isolation of the system from sources of noise had been improved, the PA signal generated had a signal to noise ratio (S/N) of about 125. Figure 16 illustrates an experiment performed after isolation was optimized and can be compared with figure 17 showing an experiment performed earlier (S/N = 8).

To determine whether the source of the remaining noise was electrical or vibrational in nature the following experiment was done. The piezo transducer was removed and the electrodes were terminated with a 50  $\Omega$  resistor. The chopper and the lock-in amplifier were on and the noise, as measured by the lock-in amplifier, was recorded as 164 nV. Activating the computer and the screen increased the noise to 170 nV. Figure 18 shows the effect of activating the room lights, the transformer for the laser, and the laser had on the electrical signal being measured. The electrical noise being measured did not increase as the items were energized, however the base level of the electrical noise may be high and requires further investigation. The measurements were repeated with the piezo transducer in place. There was an increase in the noise which indicated further acoustical dampening is required.

## Reproducibility

Reproducibility of multiple scans over the same region of ceramic material has been enhanced. Figure 19 depicts the results of three scans repeated over the same area of the ball bearing. All three scans show the same general profile but the noise in the signal is still excessive, overshadowing details that would indicate the presence of a flaw. While it is not conclusive, there is some promise of positive correlation in the results which encourages further investigation.

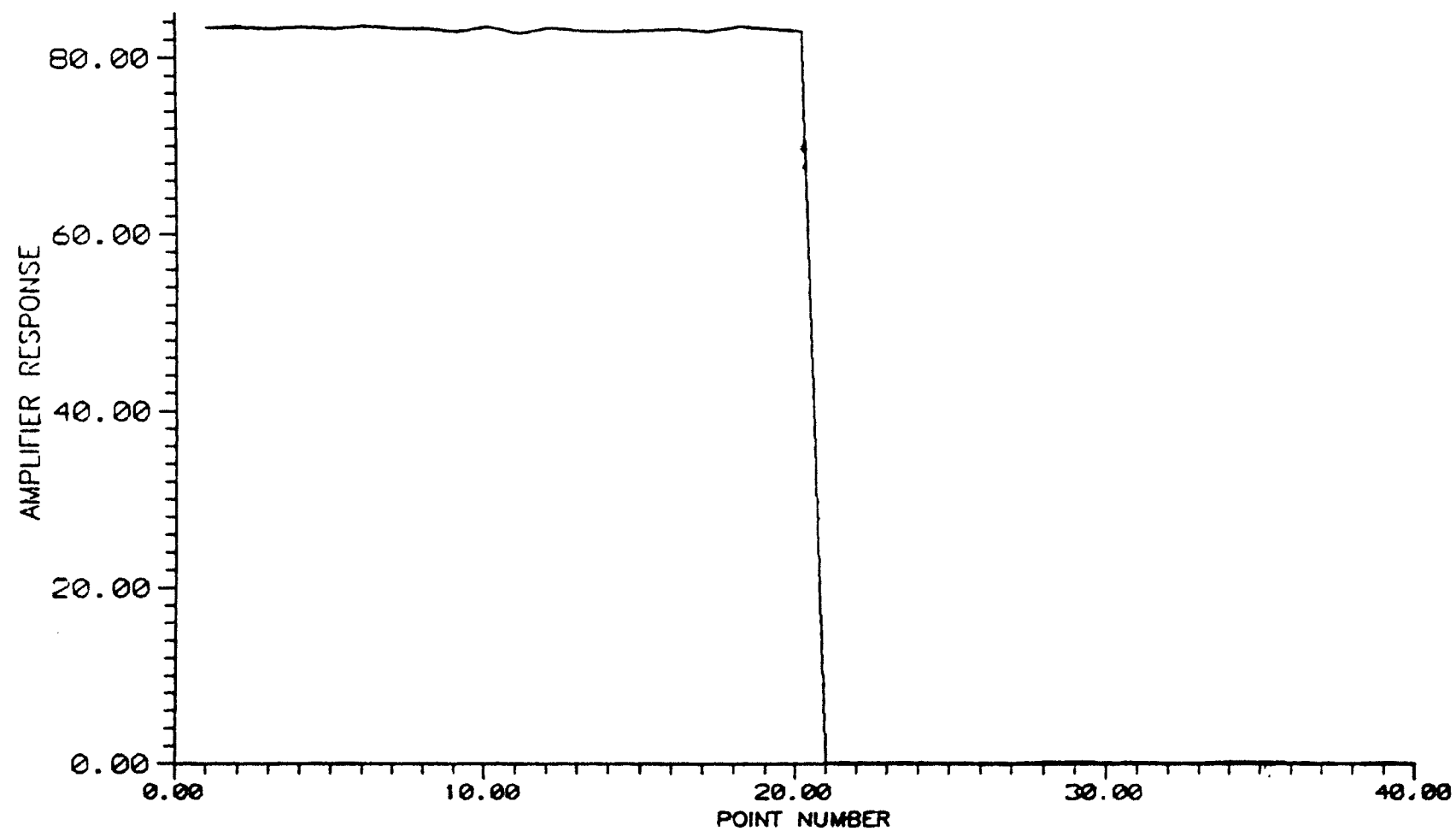


Figure 16. Experiment performed after optimizing isolation of the photoacoustic system.

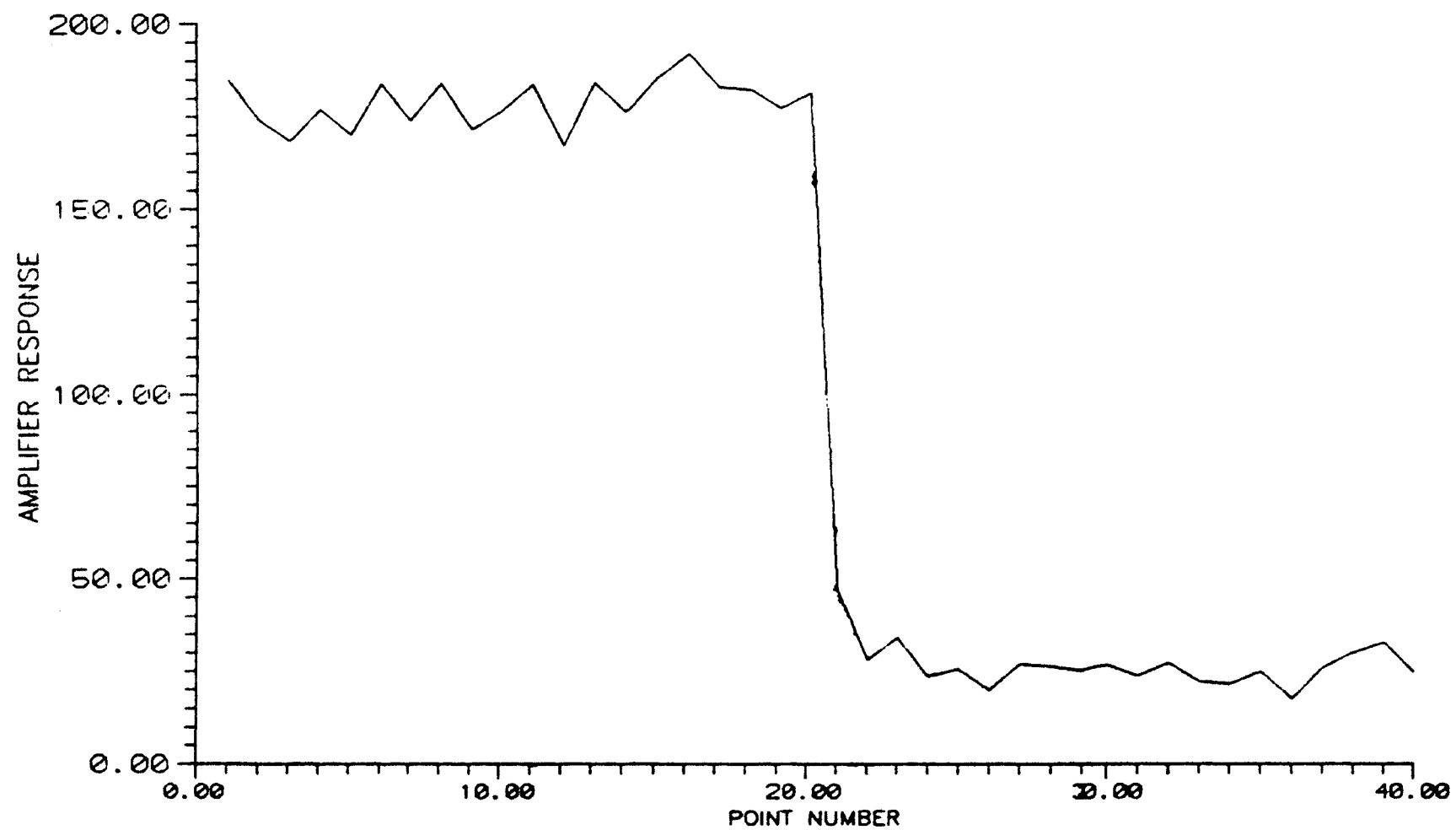


Figure 17. Experiment performed before optimizing isolation of the photoacoustic system.

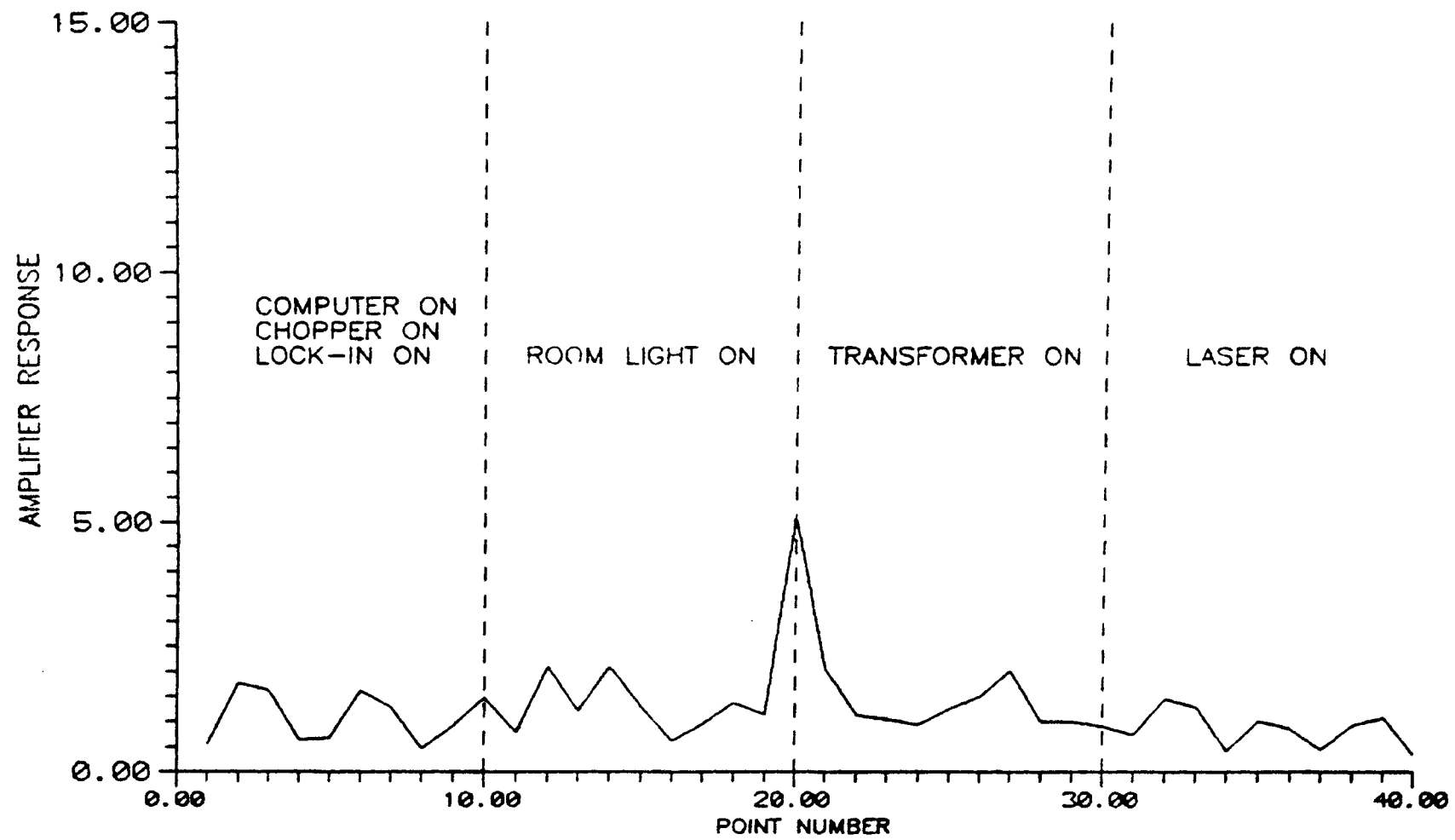


Figure 18. Experiment performed to test for addition of noise into photoacoustic system from electrical sources.

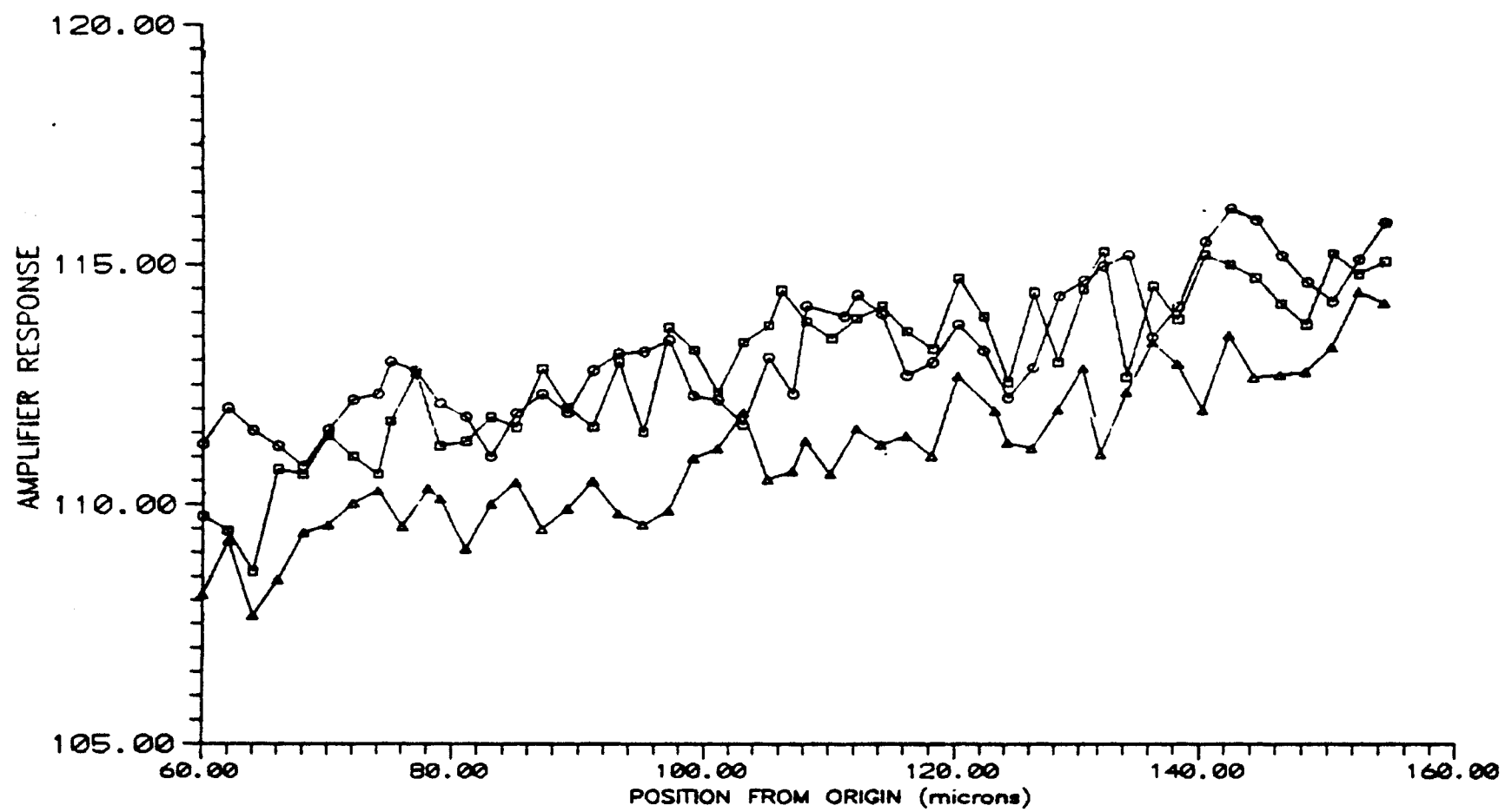


Figure 19. Three scans over a region of  $\text{Si}_3\text{N}_4$  material to verify reproducibility of photoacoustic scans.

## CHAPTER VII

### ALTERNATIVE DETECTION METHODS

#### Introduction

The signal to noise ratio (125) has not been adequate for detection of the small variations in the acoustic signal brought about by surface or subsurface flaws. Experiments will be performed with the laser operating in constant light mode to see how much the laser output is varying in intensity. If these experiments show that the stability of the laser in the current control mode is not satisfactory, then the experimental setup will be altered to monitor the intensity and normalize the data accordingly.

While it is hoped that the measures will prove adequate, it is possible that the noise will be reduced to a level to where other, as to date undetected, sources of noise may become apparent. Alternate methods of measuring the surface deformations of the material could potentially be free of acoustic noise.

#### Michelson Interferometer

The alternate heating and cooling of the ceramic surface produces periodic expansion and contraction of the material. Thermal diffusivity and chopping frequency determines the size

of the area that bulges outward upon heating and the depth of heat penetration prior to a cooling phase. The degree of bulging and contraction is determined by the thermal expansion, specific heat, thermal conductivity, and density of the material. If a particular volume has a flaw within it, the material's thermal properties are altered and there is a change in the magnitude the surfaces bulges. Optical interferometry can measure changes in a surface position on the order of fraction of a wavelength. It is anticipated that the bulging would be large enough to monitor using a Michelson interferometer.

Mounting the sample on a rigid platform firmly affixed to the optical table that the probe laser is on results in a substantial reduction of the acoustical noise. The periodic heating of the sample would be done by a high power excitation laser operating at a different wavelength than the weak continuous wave probe laser. Using two lasers provides continual observation of the surface by the probe laser while exciting the surface in a periodic manner with the strong laser. In addition, due to direct, high sensitivity interferometric observation of surface deformation, detection of the flaws is enhanced. In the proposed system, the exciting laser is chopped while the probe laser, operating at a different wavelength, is continuous and is used as a light source for the interferometer. Since the probe laser operates continuously, there is no problem with losing the image of the fringes. It is worth noting that such methods are already accepted as the most sensitive arrangement for gravitational



wave detectors and there is a lot of literature on the properties and optimization of such systems [26-32].

The optical interferometry system allows use of a feedback control system to eliminate the effects of temperature and other slow vibrational fluctuations. The experimental setup (figure 20) utilizes two lasers operating at different wavelengths, one at  $\lambda_1$  and the other at  $\lambda_2$ . The excitation beam at wavelength  $\lambda_1$  is amplitude modulated by the chopper. Mirror M1, being highly transparent to  $\lambda_1$  and highly reflective to  $\lambda_2$ , mixes the beams of the two lasers. The Michelson interferometer is created from splitter S1 (highly transparent to  $\lambda_1$  and is a 50% beam splitter for  $\lambda_2$ ), mirror M2 (highly reflective for  $\lambda_2$ ), and the specimen (acting as a reflector).

To maximize sensitivity, the lengths of the interferometer's arm should be adjusted to where measurements are made at half the maximum value of the fringe intensity (see figure 21). The reference beam is compared to the sample beam using a differential amplifier, and the output is passed through a low-pass filter. The feedback for the control system is provided by PD1 and PD2 photo diodes monitoring the intensity of the laser beam at M3 and M4. These two mirrors are 90% reflective, thus the original beam (reference) and the interferometer's beam (sample) are monitored and the difference between the signals of PD1 and PD2 is amplified and determines the adjustment of the length of the Michelson interferometer to a position corresponding to equal input signals. The low-pass filter of the control system allows for

data collection without interference from the control system and prevents the control system from responding to the changes in the surface induced by the excitation laser. The lock-in amplifier samples the fringes at a rate set by the chopper. The use of optical interferometry provides a direct measure of the PA effect. Sensitivity of this direct method should be greater than using an attached piezo.

### Infra-Red Monitoring

An alternate method of measurement would be to determine the temperature changes of the area heated by the exciting laser by an IR detector. Ideally one would use an IR detector sensitive in the 5 to 10 microns range. Detection of 10 micron radiation requires different optics than the microscope optics used to focus the laser beam on the sample since glass lenses strongly absorb the infrared radiation. A good compromise wavelength that the microscope is transparent to and that allows for observation in the anticipated temperature range is about 1.5 microns. Flaws present in the ball bearing would produce changes in the thermal characteristics of the material and the temperature of the area being observed .

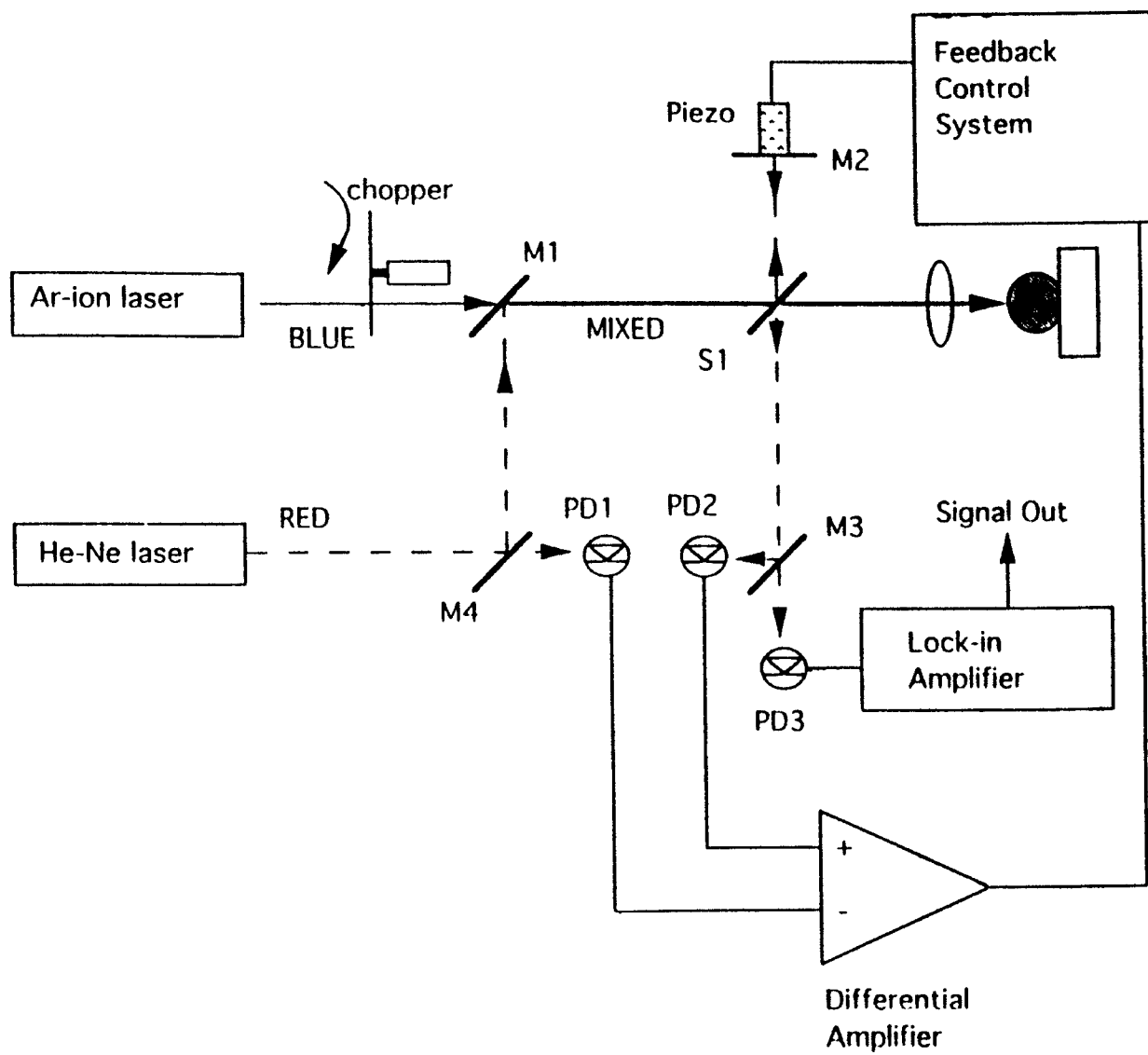


Figure 20. Block diagram of Michelson Interferometer system

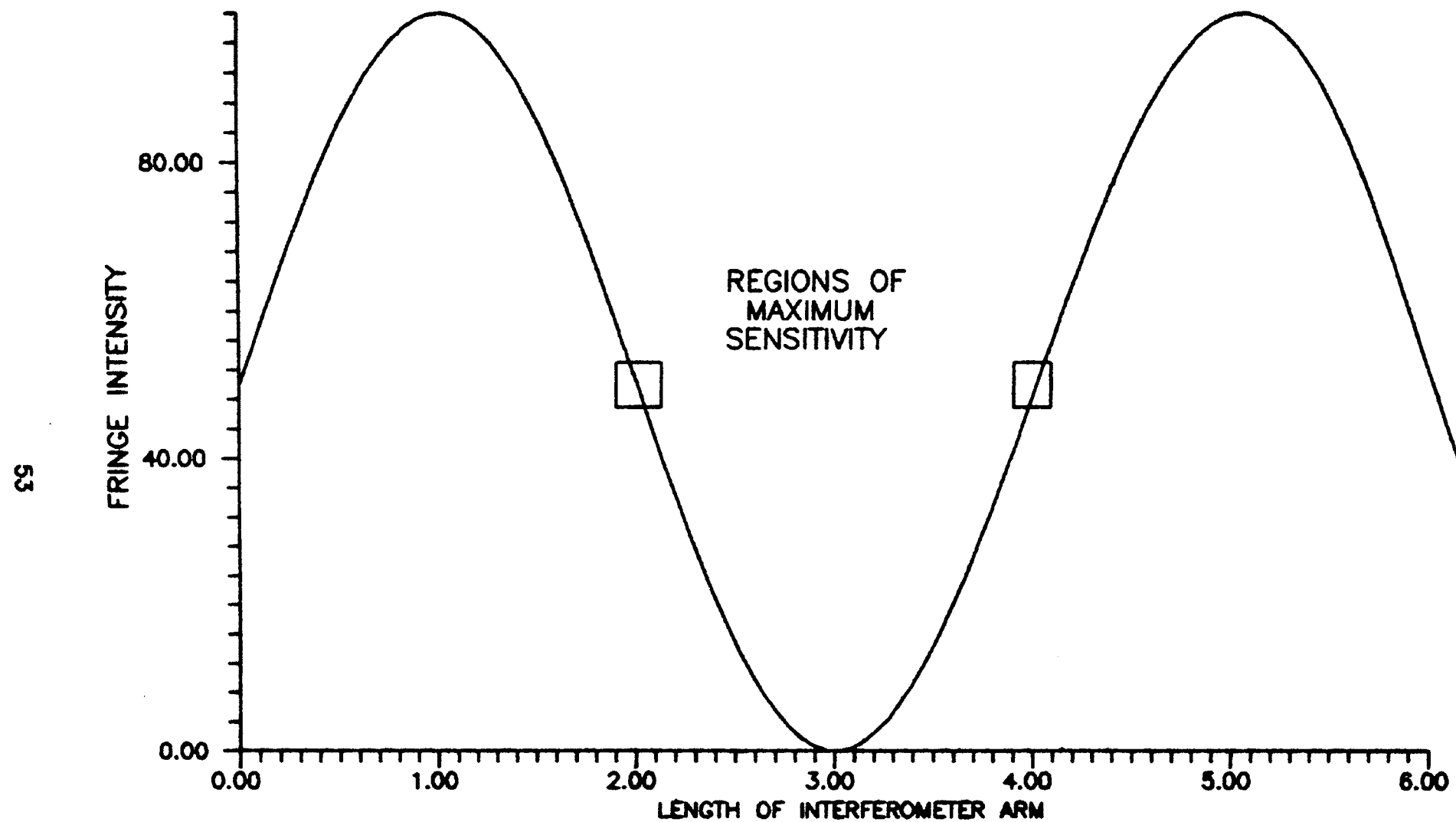


Figure 21: Diagram of the variation of fringe intensity illustrates how maximum sensitivity toward changes in the arm length  $l_2$  occurs at the half maximum point.

## CHAPTER VIII

### SUMMARY

The photoacoustic microscope is a difficult apparatus to adequately shield from sources of noise. However, once adequate isolation has been accomplished, the technique is one of very few that can observe subsurface flaws in  $\text{Si}_3\text{N}_4$  ball bearings. The size, opaque nature, round surfaces, and the grain structure of the ball bearings to be tested make other classic techniques inadequate.

The experiments performed during this study, though not conclusive, show promise of photoacoustic microscopy providing accurate data for determining the presence or absence of flaws and further study of this technique should be made. The use of alternate monitoring techniques, which provide direct measurement of the deformation of the surface or of localized heating of the ball bearing, could reduce the noise to an acceptable level. These techniques need to be explored since they also hold promise of improving the detection of flaws.

#### BIBLIOGRAPHY

1. Solomon Musikant, What Every Engineer Should Know About Ceramics, (Marcel Dekker, NY 1991) pp. 129-132.
2. S. J. Klima, Materials Evaluation, 44, 571 (1986).
3. Solomon Musikant, What Every Engineer Should Know About Ceramics, (Marcel Dekker, NY 1991) pp. 132-133.
4. Solomon Musikant, What Every Engineer Should Know About Ceramics, (Marcel Dekker, NY 1991) p. 133.
5. E. R. Generazio and D. J. Roth, Materials Evaluation, 44, 863 (1986).
6. S. J. Klima, Materials Evaluation, 44, 571 (1986).
7. Allan Rosenwaig, Photoacoustics and Photoacoustic Spectroscopy, (John Wiley & Sons, NY 1980), p.10.
8. V. P. Zharov, and V. S. Letokhov, Laser Optoacoustic Spectroscopy, (Springer-Verlag, NY 1986), pp 3-4.
9. Andrew C. Tam in Ultrasensitive Laser Spectroscopy, edited by David S. Kliger, (Academic Press, NY 1983), p. 2.
10. V. P. Zharov, and V. S. Letokhov, Laser Optoacoustic Spectroscopy, (Springer-Verlag, NY 1986), p. 72.
11. V. P. Zharov, and V. S. Letokhov, Laser Optoacoustic Spectroscopy, (Springer-Verlag, NY 1986), p. 266.
12. Solomon Musikant, What Every Engineer Should Know About Ceramics, (Marcel Dekker, NY 1991) p. 133.
13. A. G. Bell, Am. J. Sci. 20, 305 (1880)
14. Andrew C. Tam in Ultrasensitive Laser Spectroscopy, edited by David S. Kliger, (Academic Press, NY 1983), p. 2.
15. Andrew C. Tam in Ultrasensitive Laser Spectroscopy, edited by David S. Kliger, (Academic Press, NY 1983), p. 22.
16. A. Rosencwaig, Photoacoustics and Photoacoustic Spectroscopy, (John Wiley and Sons, NY 1980) p125.

## APPENDIX A

The computer program for controlling the DC mike motors, collecting the PA signal, and collecting the laser beam intensity signal is included in Appendix A. The Quick Basic program uses the I/O bus of the C-812 plug-in board provided by Physik Instrumente to exchange commands and data. The program has built in limits on the travel distance of the motors to protect the motors from damage by overdriving them.

```

DECLARE SUB GETDATA ( ) : DECLARE SUB MOVEY ( )
DECLARE SUB MOVEX ( ) : DECLARE SUB PAUSE2 (A$)
DECLARE SUB PAUSE1 (A$) : DECLARE SUB SHOWA (A$)

DECLARE SUB LETA ( ) : DECLARE SUB RTN ( )
DECLARE SUB NUM0 ( ) : DECLARE SUB NUM1 ( )
DECLARE SUB NUM2 ( ) : DECLARE SUB NUM3 ( )
DECLARE SUB NUM4 ( ) : DECLARE SUB NUM5 ( )
DECLARE SUB NUM6 ( ) : DECLARE SUB NUM7 ( )
DECLARE SUB NUM8 ( ) : DECLARE SUB NUM9 ( )

DECLARE SUB D ( ) : DECLARE SUB G ( ) : DECLARE SUB H ( )
DECLARE SUB M ( ) : DECLARE SUB N ( ) : DECLARE SUB P ( )
DECLARE SUB R ( ) : DECLARE SUB S ( ) : DECLARE SUB T ( )
DECLARE SUB W ( )

'*****

'PROGRAM "CONTROL"

'VERSION 3.2  17 DEC 1993  GHM

'THIS PROGRAM PERFORMS IBM 486 TO C-812 COMMUNICATIONS

'For use with the Photoacoustic project, this program
'controls the Physik Instrumente motor and provides
'for data collection from the A/D board.

'It requires Rev. 4.1 or higher of the C-812 firmware.

'*****

DECLARE FUNCTION fromc812$ ( )      'Function gets data from
                                   'C-812 over bus
DECLARE SUB TOC812 (DATA$)         'Subroutine sends data
                                   'to C-812 over bus

COMMON SHARED XPOS AS SINGLE, YPOS AS SINGLE
COMMON SHARED FILE AS STRING, SAMNO AS SINGLE

IBMBASE = &HD800                    'This code sets address of
IBMBASE$ = "D800"                  'C-812 board enabling computer
CONST DATA.OUT = &H3FC            'to send and receive commands
CONST data.in = &H3FE              'and data
CONST DATA.AVAIL = &H800

SCREEN 0, 1, 0, 0
VIEW PRINT
DEF SEG = IBMBASE                  'SET BASE ADDRESS TO MATCH BOARD
                                   'ADDRESS

```



```
FILE$ = FILE$ + NUFIL$
PRINT FILE$
```

```
'*****'
```

```
FOR YPOS = YST TO YFN STEP YSTP '*****
  CALL MOVEY 'controls the 2-D
  FOR XPOS = XST TO XFN STEP XSTP 'scan over an area
    CALL MOVEX 'of the surface. Subs
    CALL GETDATA 'MOVEY & MOVEX commands
    CALL NUM1 'motors to move to YPOS
    CALL G '& XPOS then the data
    CALL H 'is stored & X-motor
    CALL RTN 'goes home. The loop
    CALL PAUSE1(A$) 'moves to new XPOS &
  NEXT XPOS 'data collected. PAUSE1
  CALL NUM2 'prevents data collection
  CALL G 'prior to motor stopping.
  CALL H 'both motors GO HOME then
  CALL RTN 'move again. PAUSE2 is
  CALL PAUSE2(A$) 'same as PAUSE1(A$).
NEXT YPOS '*****
NEXT LL1
```

```
CALL G: CALL H: CALL RTN
VIEW PRINT
EXT:
CLS
PRINT "C812BUS TERMINATED"
END
```

```
SUB SHOWA (A$)
```

```
  A$ = fromc812$
  IF A$ = CHR$(255) THEN
    PRINT "NO C-812 BOARD FOUND AT "; IBMBASE$
    PRINT "PRESS F1 TO SELECT ANOTHER ADDRESS)"
    FOR xxx = 1 TO 10000: NEXT
    ' CHR$(7)
  END IF
  IF LEN(A$) > 0 THEN
    IF wide% = 1 THEN
      IF A$ = CHR$(10) OR A$ = CHR$(13) THEN
        PRINT " ";
      ELSE
        PRINT A$;
      END IF
    ELSE
      IF (A$ <> CHR$(10)) AND (A$ <> CHR$(255)) THEN PRINT A$;
    END IF
    IF A$ = CHR$(3) THEN PRINT CHR$(13);
  END IF
```

```
END SUB
```

```

SUB GETDATA      'The subroutine gets the y position, x
                  'position, the output of the lock-in,
                  'averages the output over a specified
                  'number of sample points and then dumps
                  'these parameters to a designated file.
                  'The number of sample points (SAMPNO)
                  'is set in the main program as is the
                  'filename that the data is dumped to.

```

```

FOR L = 1 TO 20: CALL SHOWA(A$): NEXT L

```

```

    'Get value for Y-axis

```

```

    CALL NUM2
    CALL T
    CALL P
    CALL RTN

```

```

    YVAL$ = ""
    DO UNTIL LEN(YVAL$) = 13
        CALL SHOWA(A$)
        YVAL$ = YVAL$ + A$
    LOOP
    YVAL$ = RIGHT$(YVAL$, 6)

```

```

    'Get value for X-axis

```

```

    CALL NUM1
    CALL T
    CALL P
    CALL RTN

```

```

    XVAL$ = ""
    DO UNTIL LEN(XVAL$) = 13
        CALL SHOWA(A$)
        XVAL$ = XVAL$ + A$
    LOOP
    XVAL$ = RIGHT$(XVAL$, 6)
    XPOST = VAL(XVAL$)
    XPOST = CINT(XPOST / 16.6667)

```

```

    'Wait FORTYFIVE sec for system to calm down

```

```

    SLEEP 45

```

```

    'Get value for Analog Channel #1

```

```

    CALL T
    CALL LETA
    CALL NUM1
    FOR L = 1 TO SAMPNO
        CALL RTN
    
```

```

        ZVAL$ = ""
        DO UNTIL LEN(ZVAL$) = 7
            CALL SHOWA(A$)
            ZVAL$ = ZVAL$ + A$
        LOOP
        ZVAL$ = RIGHT$(ZVAL$, 4)
        ZVAL = VAL(ZVAL$)
        TOTAL = ZVAL + TOTAL

NEXT L

        AVER = TOTAL / SAMNO
        PRINT XPOST, AVER, FILE$
OPEN FILE$ FOR APPEND AS #1
PRINT #1, XPOST, AVER
CLOSE

END SUB

SUB MOVEX
P1$(1) = "0": P1$(2) = "0": P1$(3) = "0": P1$(4) = "0"
P1$(5) = "0": P1$(6) = "0": P1$(7) = "0"
XPOS1$ = STR$(XPOS)

LENGTH = LEN(XPOS1$)
FOR K = 1 TO LENGTH
    P1$(K) = RIGHT$(XPOS1$, 1)
    M1 = LENGTH - K
    XPOS1$ = LEFT$(XPOS1$, M1)
NEXT K
P1$(LENGTH) = "0"
'PRINT P1$(7); P1$(6); P1$(5); P1$(4); P1$(3); P1$(2); P1$(1)

CALL NUM1: CALL M: CALL LETA
FOR K = 7 TO 1 STEP -1
    IF P1$(K) = "9" THEN
        CALL NUM9
    ELSEIF P1$(K) = "8" THEN
        CALL NUM8
    ELSEIF P1$(K) = "7" THEN
        CALL NUM7
    ELSEIF P1$(K) = "6" THEN
        CALL NUM6
    ELSEIF P1$(K) = "5" THEN
        CALL NUM5
    ELSEIF P1$(K) = "4" THEN
        CALL NUM4
    ELSEIF P1$(K) = "3" THEN
        CALL NUM3
    ELSEIF P1$(K) = "2" THEN
        CALL NUM2
    ELSEIF P1$(K) = "1" THEN

```

```

        CALL NUM1
        ELSEIF P1$(K) = "0" THEN
        CALL NUM0
        END IF
    NEXT K
    CALL RTN

    CALL PAUSE1(A$)

END SUB

SUB PAUSE1 (A$)
FOR L = 1 TO 20: CALL SHOWA(A$): NEXT L

TESTPOINT: WT$ = ""

        CALL NUM1
        CALL T
        CALL S
        CALL RTN

        DO UNTIL LEN(WT$) = 8
            CALL SHOWA(A$)
            WT$ = WT$ + A$
        LOOP

        TP1$ = RIGHT$(WT$, 4)
        TP1 = VAL(TP1$)
        IF TP1 = 0 THEN GOTO TESTPOINT

END SUB

SUB MOVEY 'this subroutine moves the Y-axis motor to a
          'specified position

P1$(1) = "0": P1$(2) = "0": P1$(3) = "0": P1$(4) = "0"
P1$(5) = "0": P1$(6) = "0": P1$(7) = "0"

YPOS1$ = STR$(YPOS)

LENGTH = LEN(YPOS1$)
FOR K = 1 TO LENGTH
    P1$(K) = RIGHT$(YPOS1$, 1)
    M1 = LENGTH - K
    YPOS1$ = LEFT$(YPOS1$, M1)
NEXT K
P1$(LENGTH) = "0"

CALL NUM2: CALL M: CALL LETA
FOR K = 7 TO 1 STEP -1
    IF P1$(K) = "9" THEN
        CALL NUM9
    
```

```

ELSEIF P1$(K) = "8" THEN
CALL NUM8
ELSEIF P1$(K) = "7" THEN
CALL NUM7
ELSEIF P1$(K) = "6" THEN
CALL NUM6
ELSEIF P1$(K) = "5" THEN
CALL NUM5
ELSEIF P1$(K) = "4" THEN
CALL NUM4
ELSEIF P1$(K) = "3" THEN
CALL NUM3
ELSEIF P1$(K) = "2" THEN
CALL NUM2
ELSEIF P1$(K) = "1" THEN
CALL NUM1
ELSEIF P1$(K) = "0" THEN
CALL NUM0
END IF

```

```

NEXT K

```

```

CALL RTN

```

```

'CALL PAUSE2(A$)

```

```

END SUB

```

```

SUB PAUSE2 (A$)

```

```

FOR L = 1 TO 20: CALL SHOWA(A$): NEXT L

```

```

TESTPOINT2: WT$ = ""

```

```

CALL NUM2
CALL T
CALL S
CALL RTN

```

```

DO UNTIL LEN(WT$) = 8

```

```

CALL SHOWA(A$)

```

```

WT$ = WT$ + A$

```

```

LOOP

```

```

TP1$ = RIGHT$(WT$, 4)
TP1 = VAL(TP1$)

```

```

IF TP1 = 0 THEN GOTO TESTPOINT2

```

```

END SUB

```

```

SUB TOC812 (data$) STATIC
'SENDS INPUT STRING TO C812

IF INSTR(data$, CHR$(27)) THEN                                'INTERRUPT C-812
    POKE DATA.OUT + 3, 32
    data$ = MID$(data$, 2)
    EXIT SUB
END IF

    IF (PEEK(DATA.AVAIL) AND 1) = 0 THEN
        POKE DATA.OUT, ASC(data$)      'SEND DATA TO C812, 3FC
        POKE DATA.OUT + 3, ASC(data$)  'SEND DATA TO C812, 3FF
        data$ = MID$(data$, 2)
    END IF
END SUB 'toc812

FUNCTION fromc812$ STATIC

'IF A CHARACTER IS AVAILABLE, THE SINGLE CHARACTER IS
'RETURNED. IF NONE AVAILABLE, AN EMPTY STRING IS RETURNED

    fromc812$ = ""

    IF (PEEK(DATA.AVAIL) AND 2) <> 0 THEN      'IF BOARD HAS DATA,
        fromc812$ = CHR$(PEEK(data.in))      'GET DATA

    END IF
END FUNCTION 'fromc812$

SUB NUM0
FOR L = 1 TO 20: CALL SHOWA(A$): NEXT L
    IF X$ = "" THEN X$ = "0"
    IF X$ <> "" THEN
        DO WHILE LEN(X$)
            CALL SHOWA(A$)
            CALL TOC812(X$)
            X$ = ""
        LOOP
    END IF
    X$ = ""
END SUB

SUB NUM1
FOR L = 1 TO 20: CALL SHOWA(A$): NEXT L
    IF X$ = "" THEN X$ = "1"
    IF X$ <> "" THEN
        DO WHILE LEN(X$)
            CALL SHOWA(A$)
            CALL TOC812(X$)
            X$ = ""
        LOOP
    END IF
    X$ = ""
END SUB

```

```

SUB NUM2
FOR L = 1 TO 20: CALL SHOWA(A$): NEXT L
  IF X$ = "" THEN X$ = "2"
  IF X$ <> "" THEN
    'PRINT X$;
    DO WHILE LEN(X$)
      CALL SHOWA(A$)
      CALL TOC812(X$)
      X$ = ""
    LOOP
  END IF
  X$ = ""
END SUB

```

```

SUB NUM3
FOR L = 1 TO 20: CALL SHOWA(A$): NEXT L
  IF X$ = "" THEN X$ = "3"
  IF X$ <> "" THEN
    DO WHILE LEN(X$)
      CALL SHOWA(A$)
      CALL TOC812(X$)
      X$ = ""
    LOOP
  END IF
  X$ = ""
END SUB

```

```

SUB NUM4
FOR L = 1 TO 20: CALL SHOWA(A$): NEXT L
  IF X$ = "" THEN X$ = "4"
  IF X$ <> "" THEN
    DO WHILE LEN(X$)
      CALL SHOWA(A$)
      CALL TOC812(X$)
      X$ = ""
    LOOP
  END IF
  X$ = ""
END SUB

```

```

SUB NUM5
FOR L = 1 TO 20: CALL SHOWA(A$): NEXT L
  IF X$ = "" THEN X$ = "5"
  IF X$ <> "" THEN
    DO WHILE LEN(X$)
      CALL SHOWA(A$)
      CALL TOC812(X$)
      X$ = ""
    LOOP
  END IF
  X$ = ""
END SUB

```

```

SUB NUM6
FOR L = 1 TO 20: CALL SHOWA(A$): NEXT L
  IF X$ = "" THEN X$ = "6"
  IF X$ <> "" THEN
    DO WHILE LEN(X$)
      CALL SHOWA(A$)
      CALL TOC812(X$)
      X$ = ""
    LOOP
  END IF
  X$ = ""
END SUB

```

```

SUB NUM7
FOR L = 1 TO 20: CALL SHOWA(A$): NEXT L
  IF X$ = "" THEN X$ = "7"
  IF X$ <> "" THEN
    DO WHILE LEN(X$)
      CALL SHOWA(A$)
      CALL TOC812(X$)
      X$ = ""
    LOOP
  END IF
  X$ = ""
END SUB

```

```

SUB NUM8
FOR L = 1 TO 20: CALL SHOWA(A$): NEXT L
  IF X$ = "" THEN X$ = "8"
  IF X$ <> "" THEN
    DO WHILE LEN(X$)
      CALL SHOWA(A$)
      CALL TOC812(X$)
      X$ = ""
    LOOP
  END IF
  X$ = ""
END SUB

```

```

SUB NUM9
FOR L = 1 TO 20: CALL SHOWA(A$): NEXT L
  IF X$ = "" THEN X$ = "9"
  IF X$ <> "" THEN
    DO WHILE LEN(X$)
      CALL SHOWA(A$)
      CALL TOC812(X$)
      X$ = ""
    LOOP
  END IF
  X$ = ""
END SUB

```



```

SUB LETA
FOR L = 1 TO 20: CALL SHOWA(A$): NEXT L
  IF X$ = "" THEN X$ = "A"
  IF X$ <> "" THEN
    DO WHILE LEN(X$)
      CALL SHOWA(A$)
      CALL TOC812(X$)
      X$ = ""
    LOOP
  END IF
  X$ = ""
END SUB

```

```

SUB D
FOR L = 1 TO 20: CALL SHOWA(A$): NEXT L
  IF X$ = "" THEN X$ = "D"
  IF X$ <> "" THEN
    DO WHILE LEN(X$)
      CALL SHOWA(A$)
      CALL TOC812(X$)
      X$ = ""
    LOOP
  END IF
  X$ = ""
END SUB

```

```

SUB G
FOR L = 1 TO 20: CALL SHOWA(A$): NEXT L
  IF X$ = "" THEN X$ = "G"
  IF X$ <> "" THEN
    DO WHILE LEN(X$)
      CALL SHOWA(A$)
      CALL TOC812(X$)
      X$ = ""
    LOOP
  END IF
  X$ = ""
END SUB

```

```

SUB H
FOR L = 1 TO 20: CALL SHOWA(A$): NEXT L
  IF X$ = "" THEN X$ = "H"
  IF X$ <> "" THEN
    DO WHILE LEN(X$)
      CALL SHOWA(A$)
      CALL TOC812(X$)
      X$ = ""
    LOOP
  END IF
  X$ = ""
END SUB

```

```

SUB M
FOR L = 1 TO 20: CALL SHOWA(A$): NEXT L
IF X$ = "" THEN X$ = "M"
IF X$ <> "" THEN
    DO WHILE LEN(X$)
        CALL SHOWA(A$)
        CALL TOC812(X$)
        X$ = ""
    LOOP
END IF
X$ = ""
END SUB

```

```

SUB N
FOR L = 1 TO 20: CALL SHOWA(A$): NEXT L
IF X$ = "" THEN X$ = "N"
IF X$ <> "" THEN
    DO WHILE LEN(X$)
        CALL SHOWA(A$)
        CALL TOC812(X$)
        X$ = ""
    LOOP
END IF
X$ = ""
END SUB

```

```

SUB P
FOR L = 1 TO 20: CALL SHOWA(A$): NEXT L
IF X$ = "" THEN X$ = "P"
IF X$ <> "" THEN
    DO WHILE LEN(X$)
        CALL SHOWA(A$)
        CALL TOC812(X$)
        X$ = ""
    LOOP
END IF
X$ = ""
END SUB

```

```

SUB R
FOR L = 1 TO 20: CALL SHOWA(A$): NEXT L
IF X$ = "" THEN X$ = "R"
IF X$ <> "" THEN
    DO WHILE LEN(X$)
        CALL SHOWA(A$)
        CALL TOC812(X$)
        X$ = ""
    LOOP
END IF
X$ = ""
END SUB

```

```

SUB RTN
FOR L = 1 TO 20: CALL SHOWA(A$): NEXT L
IF X$ = "" THEN X$ = CHR$(13)
IF X$ <> "" THEN
    DO WHILE LEN(X$)
        CALL SHOWA(A$)
        CALL TOC812(X$)
        X$ = ""
    LOOP
END IF
X$ = ""
END SUB

```

```

SUB S
FOR L = 1 TO 20: CALL SHOWA(A$): NEXT L
IF X$ = "" THEN X$ = "S"
IF X$ <> "" THEN
    DO WHILE LEN(X$)
        CALL SHOWA(A$)
        CALL TOC812(X$)
        X$ = ""
    LOOP
END IF
X$ = ""
END SUB

```

```

SUB T
FOR L = 1 TO 20: CALL SHOWA(A$): NEXT L
IF X$ = "" THEN X$ = "T"
IF X$ <> "" THEN
    DO WHILE LEN(X$)
        CALL SHOWA(A$)
        CALL TOC812(X$)
        X$ = ""
    LOOP
END IF
X$ = ""
END SUB

```

```

SUB W
FOR L = 1 TO 20: CALL SHOWA(A$): NEXT L
IF X$ = "" THEN X$ = "W"
IF X$ <> "" THEN
    DO WHILE LEN(X$)
        CALL SHOWA(A$)
        CALL TOC812(X$)
        X$ = ""
    LOOP
END IF
X$ = ""
END SUB

```

VITA

Gordon H. Miller

Candidate for the Degree of

Master of Science

Thesis: PHOTOACOUSTIC METHOD FOR NONDESTRUCTIVE TESTING  
OF CERAMIC BALL BEARINGS

Major Field: Electrical Engineering

Biographical:

Personal Data: Born in Johnson City, Tennessee, On  
November 11, 1957, the son of Harold J. and Ann  
Miller.

Education: Graduated from Madisonville High School,  
Madisonville, Tennessee in May 1975; received  
Associate of Science degree in Chemistry from  
Hiwassee College, Madisonville, Tennessee in May  
1977; received Bachelor of Arts degree in Chemistry  
from Maryville College, Maryville, Tennessee in  
December 1979. Completed the requirements for the  
Master of Science degree with a major in Electrical  
Engineering at Oklahoma State University in May  
1994.

Experience: Employed by Oak Ridge National Laboratory  
as a Senior Research Technician 1980-1992; employed  
by Oklahoma State University, Department of  
Electrical and Computer Engineering as a graduate  
research assistant 1992 to present.